

Article

Preparation and Testing of Anti-Corrosion Properties of New Pigments Containing Structural Units of Melamine and Magnesium Cations (Mg^{2+})

Miroslav Kohl *, Fouzy Alafid , Karolína Boščíková, Anna Krejčová , Stanislav Slang , Dominik Řezníček, Radim Hrdina and Andréa Kalendová

Faculty of Chemical Technology, University of Pardubice, Studentská 573, CZ-532 10 Pardubice, Czech Republic; fawzi_r@yahoo.com (F.A.); karolina.bostikova@student.upce.cz (K.B.); anna.krejцова@upce.cz (A.K.); stanislav.slang@upce.cz (S.S.); rez.dom@seznam.cz (D.Ř.); radim.hrdina@upce.cz (R.H.); andrea.kalendova@upce.cz (A.K.)

* Correspondence: miroslav.kohl@upce.cz; Tel.: +420-446-037-272

Abstract: This paper deals with the properties and testing of newly prepared organic pigments based on melamine cyanurate containing magnesium or zinc cations depending on their composition and anticorrosive properties in model coatings. Organic pigments based on melamine cyanurate with Mg^{2+} in the form of a complex differing in the ratio of melamine and cyanurate units were prepared. Furthermore, a pigment based on melamine citrate with magnesium cation Mg^{2+} , a pigment based on melamine citrate with magnesium cation, and a pigment based on melamine cyanurate with zinc cation were prepared. The properties of Mg-containing organic pigments were also compared with those of selected magnesium-containing inorganic oxide-type pigments. The above-synthesized pigments were characterized by inductively coupled plasma-optical emission spectroscopy, elemental analysis, scanning electron microscopy, and X-ray diffraction. In addition, the basic parameters that are indicative of the applicability of the pigments in the binders of anti-corrosion coatings were determined. The anti-corrosive properties of the tested pigments were verified after application to the epoxy-ester resin-based paint binder in three different concentrations: at pigment volume concentrations of 0.10%, 0.25%, and 0.50%. The anticorrosive effectiveness of pigmented organic coatings was verified by cyclic corrosion tests in a salt electrolyte fog ($NaCl + (NH_4)_2SO_4$) in an atmosphere containing SO_2 and by the electrochemical technique of linear polarization. Finally, the effect of the structure of the pigments on the mechanical resistance of the organic coatings was investigated. The results obtained showed that the new organic pigments exhibit anticorrosive properties, and at the same time, differences in performance were found depending on the structure of the pigments tested. Specifically, the results of cyclic corrosion tests and the electrochemical technique of linear polarization clearly demonstrated that synthesized pigments of the organic type based on melamine cyanurate containing magnesium or zinc cations ensure the anti-corrosion efficiency of the tested organic coatings. The highest anti-corrosion efficiency was achieved by the system pigmented with synthesized melamine cyanurate with magnesium cation ($C_{12}H_{16}MgN_{18}O_6$), whose anti-corrosion efficiency was comparable to the anti-corrosion efficiency of the tested inorganic pigment $MgFe_2O_4$, which was prepared by high-temperature solid-phase synthesis. In addition, these organic coatings achieved high mechanical resistance after being tested using the most used standardized mechanical tests.



Citation: Kohl, M.; Alafid, F.; Boščíková, K.; Krejčová, A.; Slang, S.; Řezníček, D.; Hrdina, R.; Kalendová, A. Preparation and Testing of Anti-Corrosion Properties of New Pigments Containing Structural Units of Melamine and Magnesium Cations (Mg^{2+}). *Coatings* **2023**, *13*, 1968. <https://doi.org/10.3390/coatings13111968>

Academic Editor: Florina Branzoi

Received: 19 October 2023

Revised: 14 November 2023

Accepted: 17 November 2023

Published: 19 November 2023



Copyright: © 2023 by the authors. Licensee MDPI, Basel, Switzerland. This article is an open access article distributed under the terms and conditions of the Creative Commons Attribution (CC BY) license (<https://creativecommons.org/licenses/by/4.0/>).

Keywords: anti-corrosion pigment; paint; organic coating; corrosion test; melamine unit

1. Introduction

The essence of corrosion inhibition using inhibitors lies in the reduction in the substance with oxidative properties and the formation of a protective film of reaction products

of the metal with the inhibitor [1]. These substances help prevent corrosion by increasing the likelihood of a chemical reaction that can form a protective coating on the surface of the metal or otherwise disrupt the chemical reaction between the metal and the corrosive environment. In the case of anti-corrosion pigments for paints, it also depends on the ease with which the pigment or its active component is released into the corrosive environment. If the pigment is easily soluble, it is quickly depleted, and blisters are formed by osmotic processes [2–5]. Pigments with chemical action and complexing properties bind iron ions leaving the metal surface during corrosion in the form of coordination compounds, and through further reactions with atmospheric oxygen, they then create a film that blocks the activity of the anodic sites of corrosion cells (for example phosphates, molybdates) [6,7]. The group of ecologically harmless pigments includes not only phosphates, molybdates, and silicates or organically modified silicate but also oxides and mixed metal oxides. Oxides and mixed oxides of metals in micro or nanoparticle form are among anti-corrosion pigments that have been relatively little used so far [8–13]. For example, spinel-type pigments, which are also investigated, include a large group of mixed oxides of the general empirical formula AB_2O_4 with a crystal structure derived from the spinel mineral [14–16]. Environmental safety predetermines this type of pigments as a replacement for toxic anti-corrosion pigments [17].

In the area of temporary protection against corrosion of metal products, there are many types of organic compounds, referred to as organic corrosion inhibitors, when in the past, there were attempts to use these corrosion inhibitors in coatings instead of anti-corrosion pigments [18]. From this point of view, a large number of different substances were investigated, which were assumed to be able to replace or synergistically complement anti-corrosion inorganic pigments in basic anti-corrosion coatings [19,20]. Among the ecologically suitable organic pigments, e.g., magnesium azelate, lignin, salts of pelargonic acid, or salts of other organic acids, which are formed during drying of oil binders or binders modified with drying oils, have shown promise in the past as components affecting the anti-corrosive properties of primers [21]. Long-term organic inhibitors are water-insoluble compounds that are added to anti-corrosion coating systems at a higher concentration than temporary protection inhibitors but significantly lower compared to conventional anti-corrosion pigments. This enables a certain freedom in formulation, whereby new types of protective systems can be created. Their activity depends on the concentration, so it is necessary to find its optimal value [3,22].

In the area of coatings, organic pigments are mainly used in combination with inorganic pigments to strengthen their function in the first phase of the corrosion action, to improve anodic protection, and subsequently to create a synergistic effect. Low solubility in water is an important criterion for their application in a coating for long-term protection [23,24]. Too high a solubility of these substances in water would lead to blistering and delamination [25]. New types of organic pigments with anti-corrosion properties include some types of perylene pigments [24,26]. Another new type of organic pigments with the possibility of future application in anti-corrosion coatings could be pigments based on the structural compounds of melamine and other organic compounds [27]. Due to their structure, these substances can have a positive effect on the structure of the polymer film. Due to the content of Mg and Zn, they could show a favorable effect on the chemical and electrochemical action of pigments in the paint binder at the metal–organic coating interface [28]. Melamine cyanurate (MCy) is essentially a hydrogen complex between melamine and cyanuric acid (Figure 1) [29]. MCy is also called “white graphite” in the literature and is characterized by very good lubrication properties because it has a graphite structure (a two-dimensional network of hydrogen bonds). Melamine cyanurate, also known as melamine–cyanuric acid addition compound or melamine–cyanuric acid complex, also 1,3,5-triazine-2,4,6-trione, is a crystalline complex formed by a mixture of melamine and cyanuric acid in the ratio 1:1. MCy is highly symmetric hydrogen-bonded two-dimensional array of cyanuric acid and melamine forming cocrystal [29]. This substance is not a salt, although it is referred to by the systematic name melamine cyanurate (IUPAC name 1,3,5-

triazine-2,4,6(1H,3H,5H)-trione + 1,3,5-triazine-2,4,6-triamine (1:1). MCy is used in some polymers using its relatively good thermal stability, as a flame retardant, e.g., in polyamide 6 and polyamide 66 [30–32].

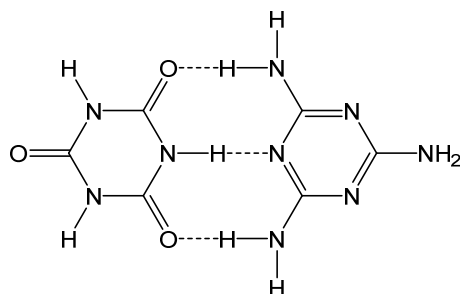


Figure 1. Melamine–cyanurate structure [33].

2. Materials

Cyanuric acid, magnesium hydroxide, melamine, orotic acid, zinc oxide and xylene mixture of isomers (Merck KGaA, Darmstadt, Germany), citric acid, calcium carbonate (Lach-ner s.r.o.; Neratovice, Czech Republic), red hematite (ferric oxide, α -Fe₂O₃, trade name: Bayferrox 160M, Lanxess GmbH, Köln, Germany), titanium dioxide (TiO₂, structure: anatase; Precheza a.s., Prerov, Czech Republic), and magnesium carbonate (MgCO₃, structure: magnesite; Lachema a.s., Brno, Czech Republic). Nitric acid (Penta Chrudim, Czech Republic, purity PP). Epoxy ester resin WorléeDur D46 and sicative Valirex Mix 835 D60 (3P-CHEM s.r.o., Zbůch, Czech Republic). Loctite EA 9466 adhesive for pull-off tests (Ulbrich Hydroautomtic s.r.o., Brno, Czech Republic).

3. Experimental

3.1. Synthesis of Organic Pigments

The subject of this work was to synthesize selected organic pigments with structural elements of melamine units containing Mg. The synthesis was carried out according to the proposed and verified procedures in a solvent environment under the given temperature conditions. Melamine cyanurate, as part of the structure of the new pigment, is a complex formed by a mixture of melamine and cyanuric acid. The stability of the complex is ensured by hydrogen bonds between the two compounds. Magnesium was chosen because of its proven positive effect on the anti-corrosion properties of many types of pigments, and it is also more environmentally acceptable than zinc [34,35].

These organic pigments with supposed anti-corrosion properties were prepared by the reaction of melamine, cyanuric acid and other substances to form a complex layered (sandwich) structure. Furthermore, pigments were similarly prepared by reacting melamine, orotic acid and citric acid together with magnesium hydroxide and zinc hydroxide.

A new set of five organic white pigments were prepared (Pigment1–Pigment5). Pigment1—pigment based on melamine cyanurate with Mg²⁺ in the form of a complex, Pigment2—pigment based on melamine cyanurate with Mg²⁺ in the form of a complex in a different ratio of melamine and cyanurate units to the Mg²⁺ cation, Pigment3—pigment based on melamine citrate with magnesium cation, Pigment4—pigment based on melamine orotic acid with magnesium cation, and Pigment5—pigment based on melamine cyanurate with zinc cation. The pigment based on melamine cyanurate with Mg²⁺ cation (Pigment1) differed from the pigment based on melamine cyanurate with Mg²⁺ (Pigment2) in the number of melamine and cyanurate units. One melamine and one cyanide unit were found in Pigment1, while two melamine and two cyanide units were found in Pigment2.

3.1.1. Synthesis of Melamine Cyanurate with Magnesium Cation C₆H₇MgN₉O₃—Pigment1

Melamine (12.6 g, 99.0 mmol) was mixed with water (150 cm³) and Mg(OH)₂ (5.8 g, 99.0 mmol) was added under the stirring. Then, after cyanuric acid (12.9 g, 99.0 mmol) was added, the reaction pH value was 7–8. The reaction mixture was then vigorously stirred at 100 °C for 2 h. When the reaction was completed, the reaction mixture was cooled at room temperature (22 °C) and the obtained white powder was dried at 140 °C (Figure 2).

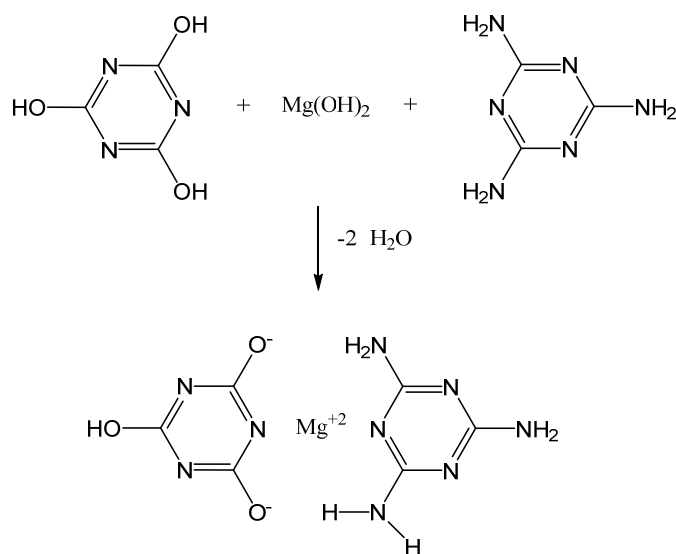


Figure 2. Synthesis equation of melamine cyanurate with magnesium cation (C₆H₇MgN₉O₃).

3.1.2. Synthesis of Melamine Cyanurate with Magnesium Cation C₁₂H₁₆MgN₁₈O₆—Pigment2

Melamine (12.6 g, 99.0 mmol) was mixed with water (150 cm³) and Mg(OH)₂ (3.0 g, 49.0 mmol) was added under the stirring. Then, after cyanuric acid (12.9 g, 99.0 mmol) was added, the reaction pH was value 7–8. The reaction mixture was then vigorously stirred at 100 °C for 2 h. When the reaction was completed, the reaction mixture was cooled at room temperature (22 °C) and the obtained white powder was dried at 140 °C (Figure 3).

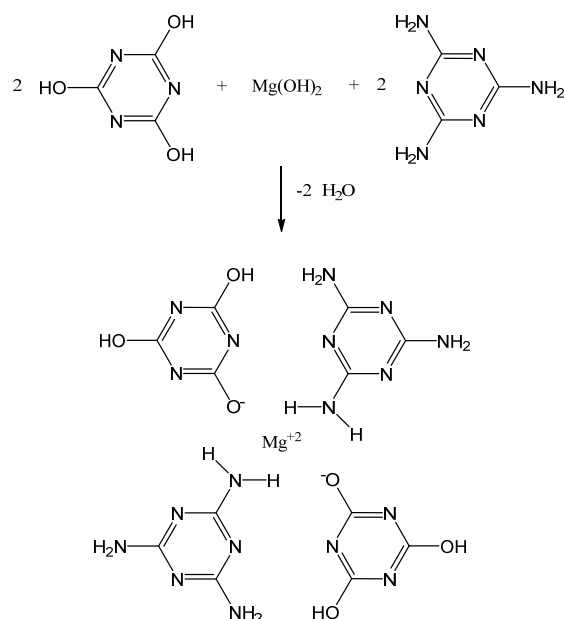


Figure 3. Synthesis equation of melamine cyanurate with magnesium cation (C₁₂H₁₆MgN₁₈O₆).

3.1.3. Synthesis of Melamine Citrate with Magnesium Cation C₁₈H₂₆MgN₁₂O₁₄—Pigment3

Melamine (12.6 g, 99.0 mmol) was mixed with water (150 cm³) and Mg(OH)₂ (3.0 g, 49.0 mmol) was added under the stirring. Then, after citric acid (19.2 g, 99.0 mmol) was added, the reaction pH value was 3–4. The reaction mixture was then vigorously stirred at 100 °C for 3 h. When the reaction was completed, the reaction mixture was cooled at room temperature (22 °C) and the obtained white powder was dried at 140 °C (Figure 4).

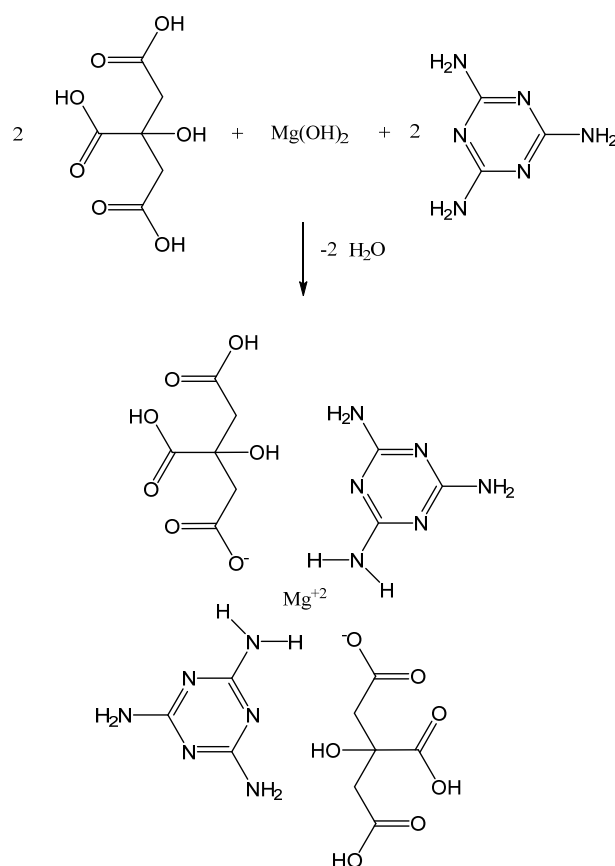


Figure 4. Synthesis equation of melamine citrate with magnesium cation.

3.1.4. Synthesis of Melamine Orotate with Magnesium Cation C₁₆H₁₈MgN₁₆O₈—Pigment4

Melamine (12.6 g, 99.0 mmol) was mixed with water (150 cm³) and Mg(OH)₂ (3.0 g, 49.0 mmol) was added under the stirring. Then, after orotic acid (17.4 g, 99.0 mmol), was added, the reaction pH value was 3–4. The reaction mixture was then vigorously stirred at 100 °C for 3 h. When the reaction was completed, the reaction mixture was cooled at room temperature (22 °C) and the obtained white powder was dried at 140 °C (Figure 5).

3.1.5. Synthesis of Melamine Cyanurate with Zinc Cation C₁₂H₁₆ZnN₁₈O₆—Pigment5

As a comparison to organic pigments containing Mg²⁺, a pigment with Zn²⁺ was synthesized. Cyanuric acid (12.9 g, 99.0 mmol) was mixed with water (150 cm³), stirred and heated, and zinc oxide (4.1 g, 50.0 mmol) was added while stirring. Then, a suspension of melamine (12.6 g, 99.0 mmol) and water (100 cm³) was added, the reaction mixture was then vigorously stirred at 100 °C for 2 h, cooled, and the filtrate pressed cake was dried at 140 °C (Figure 6).

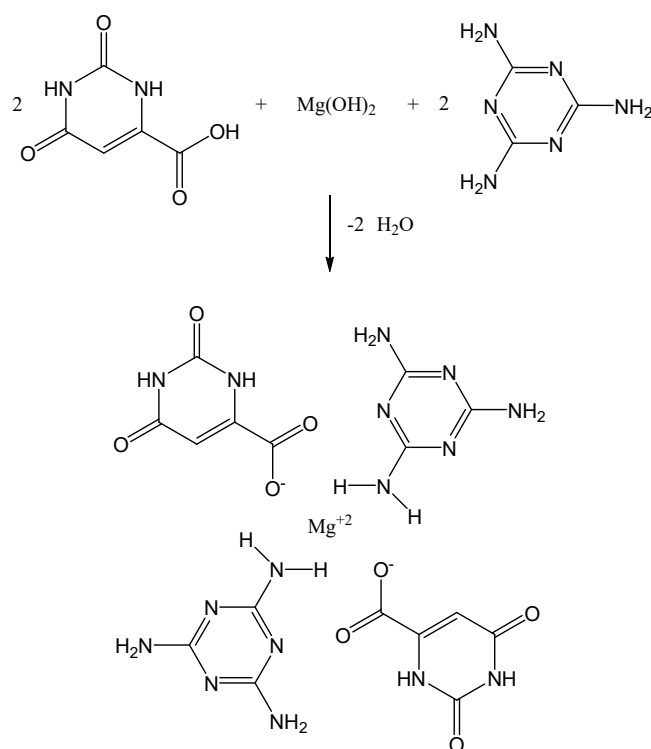


Figure 5. Synthesis equation of melamine orotate with magnesium cation.

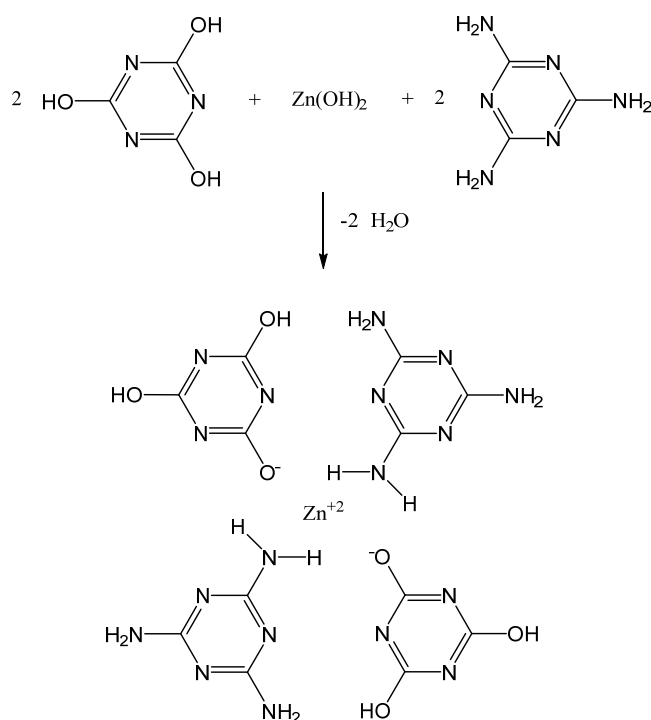


Figure 6. Synthesis equation of melamine cyanurate with zinc cation.

3.2. Synthesis of Inorganic Pigments Based on Mixed Oxides—Pigment6 and Pigment7

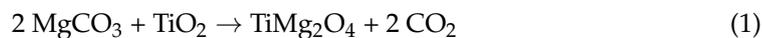
As comparison pigments to organic pigments, inorganic-type pigments based on mixed oxides were synthesized, which have already been proven to have anti-corrosion properties in previous works (Table 1) [14,15,36]. Magnesium titanium dioxide TiMg_2O_4 (Pigment6) and magnesium iron oxide MgFe_2O_4 (Pigment7) were prepared by high-temperature solid-phase synthesis of a homogenized mixture of starting materials at a

temperature of 1180 °C. Subsequently, the calcinates were adjusted to the form necessary for application in the binder of paint materials by washing, grinding in a grinding bowl (zirconium oxide), using grinding balls (corundum) in planetary mono mill Pulverisette 6 (Fritsch GmbH, Weimar, Germany), and drying at 110 °C [37,38]. The initial mixture for magnesium titanium dioxide (TiMg_2O_4) was composed of magnesium carbonate (MgCO_3) and titanium dioxide (TiO_2) of the anatase type, which were homogenized in the ratio according to the equations in Equation (1). The initial mixture for magnesium iron oxide (MgFe_2O_4) was composed of magnesium carbonate (MgCO_3) and hematite (Fe_2O_3), which were homogenized in the ratio according to the equations in Equation (2).

Table 1. Synthesized and tested pigments.

Designation	Compound	Chemical Formula	Molecular Weight [g·mol ⁻¹]	Theoretical Content of Metal (Mg/Zn) [%]
Organic pigment				
Pigment1	Melamine cyanurate/ Mg^{2+}	$\text{C}_6\text{H}_7\text{MgN}_9\text{O}_3$	277.48	8.76
Pigment2	Melamine cyanurate/ Mg^{2+}	$\text{C}_{12}\text{H}_{16}\text{MgN}_{18}\text{O}_6$	532.68	4.56
Pigment3	Melamine citrate/ Mg^{2+}	$\text{C}_{18}\text{H}_{26}\text{MgN}_{12}\text{O}_{14}$	658.77	3.69
Pigment4	Melamine orotate/ Mg^{2+}	$\text{C}_{16}\text{H}_{18}\text{MgN}_{16}\text{O}_8$	583.70	4.14
Pigment5	Melamine cyanurate/ Zn^{2+}	$\text{C}_{12}\text{H}_{16}\text{ZnN}_{18}\text{O}_6$	573.75	11.40
Inorganic pigment				
Pigment6	Magnesium titanium dioxide	TiMg_2O_4	120.17	20.23
Pigment7	Magnesium iron oxide	MgFe_2O_4	199.99	12.15
Comparative substance				
Pigment8	Titanium dioxide	TiO_2	79.87	-

Red hematite ($\alpha\text{-Fe}_2\text{O}_3$) was selected as the starting source of Fe^{3+} cations for the synthesis of the next type of oxidic spinel pigment, ferrite (MgFe_2O_4). Another pigment of the oxidic type, whose primary particles generally possess an isometric shape TiMg_2O_4 , was synthesized using titanium oxide as the source of tetravalent cations (TiO_2). Magnesium carbonate (MgCO_3) served as the source of Mg^{2+} cations. Magnesium was selected in order to make use of their favorable contribution to the pigment's chemical anti-corrosion behavior. The reactions leading to the formation of pigments are shown in Equation (1) and Equation (2).



3.3. Identification of Products of Synthesis by Analytical Methods

3.3.1. Inductively Coupled Plasma-Optical Emission Spectroscopy (ICP-OES)

Using inductively coupled plasma-optical emission spectroscopy (ICP-OES), magnesium and zinc were determined. The sample was decomposed in a Speedwave Xpert microwave mineralizer (Berghof, Tübingen, Germany). The sample was precisely weighed at 0.1 to 0.2 g, 7 mL of nitric acid was then added, and it was allowed to react for 20 min in an open vessel before being decomposed (170 °C for 15 min, 200 °C for 20 min). The mineralized sample was then diluted to a final amount of 50 mL.

Using an inductively coupled plasma-optical emission spectrometer Integra 6000 (GBC, Dandenong, VIC, Australia) fitted with a concentric nebulizer and cyclonic spray chamber (both Glass Expansion, Melbourne, Victoria, Australia), the determination of both elements in the mineralized sample was carried out at the spectral lines of Mg II 280.270 nm and Zn I 213.856 nm. The following were the working conditions for the ICP-

OES analysis: The sample flow rate was $1.5 \text{ mL}\cdot\text{min}^{-1}$, the plasma power was 1000 W, the plasma, external, and sample gases were 10, 0.6, and $0.65 \text{ L}\cdot\text{min}^{-1}$, the observation height was 6.5 mm, and the signal was read and the background correction was set using three repeated measurements at 1 s. Standard solutions of zinc and magnesium $1 \text{ g}\cdot\text{dm}^{-3}$ (SCP, Science, Clark Graham, Baie D'Urfé, QC, Canada) that are available commercially were used to create calibration standards ranging from 10, 5, 1, 0.5 to $0.1 \text{ mg}\cdot\text{dm}^{-3}$. The limits of detection (concentration equal to three times the standard deviation of noise in place of background correction) for both elements were around $2 \mu\text{g}\cdot\text{dm}^{-3}$, while the limit of detection for the entire analytical procedure, with respect to how the sample was prepared for analysis (0.05 g and 50 mL sample weight), was $2 \text{ mg}\cdot\text{kg}^{-1}$. The typical repeatability of the device measurement expressed as a relative standard deviation is 1–2%.

3.3.2. Elemental Analysis

A Flash 2000 CHNS Elemental Analyzer (Thermo Fisher Scientific, Milan, Italy) was used to conduct elemental studies of synthesized pigments.

3.3.3. SEM and EDX Measurements of Pigments

The scanning electron microscopy (SEM) scans and elemental composition data (EDX) of studied pigments were obtained using a LYRA 3 (Tescan, Brno, Czech Republic) scanning electron microscope equipped with an Aztec X-Max 20 EDS analyser (Oxford Instruments, Oxford, UK). Samples were coated with a 20-nm carbon conductive layer (ACE 200, Leica, Wetzlar, Germany) and measured on five $300 \times 300 \mu\text{m}^2$ areas at 20 kV of accelerating voltage. The results were averaged, and the error bars represent standard deviations of measured values. The pigments were coated with 18 nm of a gold conductive layer as well, and SEM scans of the studied samples were acquired at 10 kV of acceleration voltage. Determination of the metal content in the tested pigments by the SEM-EDS method was carried out with an accuracy of ± 0.5 –1%.

3.3.4. X-ray Diffraction

A D8 ADVANCE X-ray diffractometer (Bruker AXS, Karlsruhe, Germany) equipped with a vertical-goniometer (radius = 217.5 mm) was used to measure powder diffractograms. An X-ray tube with a Cu anode ($U = 40 \text{ kV}$, $I = 30 \text{ mA}$; $\lambda = 1.5418$), a scintillation Na(Tl)I detector, and a graphite secondary monochromator are all included in the goniometer. The measurements for the diffracted radiation intensity were made at room temperature in the 2 – 50° range with a 0.02° step and a reading length of 5 s/step.

3.4. Determination of Physico-Chemical Properties of Prepared Organic and Inorganic Pigments

The prepared organic and inorganic pigments were characterized using parameters important for application in binder components, such as oil absorption (determined by “pestle–mortar” method) and density (determined by Micromeritics AutoPycnometer 1340 (Norcross, GA, USA)), when based on these determined parameters the critical pigment volume concentration (CPVC) of the individual studied pigments was calculated [39,40].

3.5. Formulation, Preparation, and Application of Model Paint Materials

Solvent-based epoxy ester resin with the following basic parameters was used as a binder for the formulation of model paint materials: composition oil—40%, EP resin—60%, color DIN ISO 4630, Gardner—max. 10, acid value DIN EN ISO 2114: max. 4 [mgKOH/g], viscosity, rheometer, 23°C , C 60/2, 50 s: 3.6 – $4.8 \text{ Pa}\cdot\text{s}^{-1}$. Epoxy ester resin with the commercial name WorléeDur D 46 (3P-CHEM s.r.o., Zbůch, Czech Republic) was used as a binder and for the preparation of model paint. The expected anti-corrosion properties of the tested pigments were verified after the application of individual pigments in used resin at three different concentrations ($\text{PVC}_{\text{pig.}} = 0.10\%$, 0.25% and 0.50%). The prepared systems were additionally supplemented with inert substances (TiO_2 and CaCO_3) to ensure a constant proportion of solids in the prepared

systems, when the parameter $Q = 3.50\%$. Individual model paint materials were prepared using a Dissolver-type system (Dispermat[®] CN30-F2, VMA-Getzmann GMBH, Reichshol, Germany) at 3500 rpm/40 min using dispersing balls with a diameter of 2.85–3.45 mm (3P-CHEM s.r.o., Zbůch, Czech Republic). Valirex Mix 835 D60 (3P-CHEM s.r.o., Zbůch, Czech Republic) was applied to the model paints as a drying agent in the amount recommended by the manufacturer of the resin used (specifically 0.1% calculated on 100% alkyd resin). The drying agent is a mixture of cobalt, calcium and zirconium carboxylates in white spirit D60 with a total metal content of 8.8%. The viscosity of the prepared model paints was adjusted using xylene solvent.

The prepared model paint materials were applied to glass panels and steel panels Q-Panel standard test substrates (Q-Lab Corporation, Cleveland, OH, USA), when type S-46 was used for cyclic corrosion tests, type ZQD-SP-104171 was used for mechanical tests, and type QD-24 was used for electrochemical measurements. Individual panels were prepared according to ISO 1514 and then model paint materials were applied to them by 4-sided applicator ZFR 2040.8050 (Zehntner GmbH Testing Instruments, Sissach, Switzerland). To study the physical, mechanical and electrochemical properties of organic coatings, single-layer coating films were prepared, while two-layer systems were prepared to study the corrosion properties of coating films. Measurement of the dry thickness of the prepared organic coatings applied to steel panels was carried out according to ISO 2808 using a magnetic thickness gauge (byko-test 8500 premium Fe/Nfe, BYK Additives & Instruments, Wesel, Germany), whereas the dry thickness of paint films applied to glass panels was determined using a dial thickness gauge (Schut-20, Schut Geometrische Meettechniek B.V., Groningen, The Netherlands) according to ISO 2808. Samples of organic coatings intended for testing using mechanical, electrochemical and corrosion tests were conditioned before these tests in an air-conditioned room at a temperature of 23 ± 2 °C and a humidity of $45 \pm 5\%$ for a period of 30 days. The samples intended for cyclic corrosion tests were provided with a vertical section 80 mm long according to ISO 2409. The sections were made with a DIN Scratching Tool Elcometer 1538 with 1mm cutter (Elcometer, Manchester, UK), described in ISO 12944-6.

3.6. Mechanical Properties of the Studied Organic Coatings

The mechanical properties of the studied organic coatings were performed according to the procedures specified in the standards using the appropriate types of equipment. The relative surface hardness according to ISO 1522 was performed using a BYK-Gardner Byko-Swing (5867), Persoz Hardness Tester for Coatings (BYK-Gardner GmbH, Geretsried, Germany). The test degree of adhesion according to ISO 2409 was performed using Elcometer 1542 Cross Hatch Adhesion Tester (Elcometer, Manchester, UK). A rapid-deformation (impact resistance) test according to ISO 6272 was performed using Elcometer 1615 Variable Impact Tester (Elcometer, Manchester, UK). Bend test (cylindrical mandrel) according to ISO 1519 was performed using Elcometer 1500 Cylindrical Mandrel on a Stand (Elcometer, Manchester, UK). A cupping test according to ISO 1520 was performed using Elcometer 1620 Cupping Tester (Elcometer, Manchester, UK). The pull-off test for adhesion according to ISO 4624 was performed using a COMTEST[®] OP3P (Roklan-electronic s.r.o., Prague, Czech Republic).

3.7. Determination of pH and Specific Electrical Conductivity and Corrosion Loss from Aqueous Extracts of Pigments and of Loose Paint Films

As part of this experimental technique, the pH and specific electrical conductivity (λ) of 10% aqueous extracts of pigments (pH_p and λ_p) and loose paint films at $PVC_{pig} = 0.50\%$ (pH_f and λ_f) were studied for 28 days using procedures derived from ISO 787-9 and ISO 787-14 standards using a pH meter WTW 320, (Labexchange-Die Laborgerätebörse GmbH, Burladingen, Germany) and using a conductometer Handylab LF1 (Schott-Geräte GmbH, Landshut, Germany). Both devices were calibrated before the determinations using the respective calibration solutions supplied by the manufacturers of the devices. After 28 days,

the individual filtrates were used to determine the corrosion loss (K_{mp} and K_{mf}) after the seven-day exposure of the steel panels in these filtrates and the losses expressed as percentages by weight in relation to the weight loss of the steel in the distilled water used (X_{rel-p} and X_{rel-f}) [41].

3.8. Laboratory Corrosion Tests for Determining Anti-Corrosion Properties of Organic Coatings and Evaluation of Results after Corrosion Tests

The corrosion test in salt spray prepared from a diluted electrolyte of 0.05 wt.% sodium chloride and 0.35 wt.% ammonium sulfate (referred to as the Prohesion test) was performed according to the procedure derived from the ASTM G 85 standard (procedure A5) in a testing chamber SKB 400 A-TR-TOUCH (Gebr. Liebisch GmbH & Co. KG, Bielefeld, Germany). The test took place in repeated twelve-hour cycles (10 h of salt spray at a temperature of 35 °C, 1 h of humidity at a temperature of 40 °C and 1 h of drying at a temperature of 23 °C). The studied samples of paint films were exposed to this corrosion test for 960 h.

The corrosion test in a humid atmosphere containing SO₂ was performed according to ISO 22479 in a testing chamber KB 300A (Gebr. Liebisch GmbH & Co. KG, Bielefeld, Germany). The test took place in repeated twenty-four-hour cycles (8 h humidity with SO₂ content (dosed 1000 mL of SO₂ into a 300 L chamber) at a temperature of 38 °C and 16 h drying at a temperature of 23 °C and a humidity of less than 75%). The studied samples of paint films were exposed to this corrosion test for 960 h.

The evaluation of corrosion parameters after both corrosion tests took place after 40 cycles (480 h exposure) and then after 80 cycles, i.e., after 960 h exposure according to ASTM D 714-87 Standard Test Method for Evaluating Degree of Blistering of Paints; and ASTM D 610-85 Method for Evaluating Degree of Rusting on Painted Steel Surfaces; and ASTM D 1654-92 Standard Test Method For Evaluation of Painted or Coated Specimens Subjected To Corrosive Environments.

3.9. Electrochemical Measurement Linear Polarization

A multichannel potentiostat/galvanostat VSP-300 (Bio-Logic, Seyssinet-Pariset, France) was used to measure the polarization curves of the studied organic coatings. Evaluation of the polarization curves was performed using EC-Lab[®] software V10.23 from 2012. The samples were exposed to 1 M NaCl solution in a Galvanic cells (Bio-Logic, Seyssinet-Pariset, France), in which a saturated calomel electrode and a platinum working electrode were also placed. An area of 1 cm² of the individual studied organic coatings was polarized across the range from −10 mV EOC^{−1} to +10 mV EOC^{−1} at a rate of 0.166 Mv·s^{−1}.

4. Results and Discussion

4.1. Characterization and Structure of Synthesized Organic and Inorganic Pigments

The prepared organic pigments with expected anticorrosive properties were characterized by analytical methods. Specifically, there were four organic pigments containing magnesium (Pigment1–Pigment4) and one organic pigment containing zinc (Pigment5) and two inorganic pigments (Pigment6–Pigment 7). The results of the analytical techniques are shown in Table 2. Characterization of samples using elemental analysis and OES-ICP technique was performed only for organic pigments while the SEM-EDS technique was used to study the distribution of metals in organic samples and to determine the content of metals in inorganic samples.

The measured results of the elemental analysis correspond to the calculated results for individual organic pigments. Five types of organic pigments were characterized using the OES-ICP technique, where the results of this technique confirm the correctness of the syntheses of individual organic pigments. A high proportion of magnesium was found in the Pigment1 C₆H₇MgN₉O₃ (7.70%) and in the Pigment2 C₁₂H₁₆MgN₁₈O₆ (4.33%), which is a prerequisite for its anti-corrosion. The zinc content in the C₁₂H₁₆ZnN₁₈O₆ Pigment5 determined by this technique exactly corresponded to the theoretical amount of zinc in

this pigment. The presence of metal and its uniform distribution were confirmed using the SEM-EDS technique. A higher magnesium content compared to organic pigments was confirmed by the method for inorganic pigments, which also results from the structure of these pigments, when the magnesium content of the TiMg_2O_4 Pigment6 was determined to be 15.6%, while the magnesium content of the MgFe_2O_4 Pigment7 was determined to be 11.6%. Low concentrations of Al or Si demonstrated by the SEM-EDS technique in inorganic samples originate from the grinding bowl or grinding balls.

Table 2. Characterization of synthesized pigments.

Designation	Compound	Chemical Formula	Elemental Analysis (Calc./Found) [%]	SEM-EDS [hm.%]	Content of Metal (Mg/Zn) [%]
Pigment1	Melamine cyanurate/ Mg^{2+}	$\text{C}_6\text{H}_7\text{MgN}_9\text{O}_3$	C: 25.97/23.27 H: 2.54/3.44 N: 45.43/34.69	C: 27.2 ± 0.8 Mg: 4.1 ± 0.2 N: 43.0 ± 0.7 O: 25.7 ± 0.7	7.70
Pigment2	Melamine cyanurate/ Mg^{2+}	$\text{C}_{12}\text{H}_{16}\text{MgN}_{18}\text{O}_6$	C: 27.06/25.44 H: 3.03/3.42 N: 47.33/38.04	C: 28.1 ± 1.0 Mg: 2.5 ± 0.1 N: 45.7 ± 0.7 O: 23.7 ± 0.4	4.33
Pigment3	Melamine citrate/ Mg^{2+}	$\text{C}_{18}\text{H}_{26}\text{MgN}_{12}\text{O}_{14}$	C: 32.82/30.63 H: 3.98/4.34 N: 25.51/30.92	C: 32.5 ± 0.6 Mg: 2.0 ± 0.1 N: 38.2 ± 0.6 O: 27.3 ± 0.6	2.59
Pigment4	Melamine orotate/ Mg^{2+}	$\text{C}_{16}\text{H}_{18}\text{MgN}_{16}\text{O}_8$	C: 32.75/30.80 H: 3.09/3.61 N: 38.20/29.96	C: 31.8 ± 0.8 Mg: 2.9 ± 0.1 N: 32.0 ± 0.2 O: 33.4 ± 0.7	3.39
Pigment5	Melamine cyanurate/ Zn^{2+}	$\text{C}_{12}\text{H}_{16}\text{ZnN}_{18}\text{O}_6$	C: 25.12/23.71 H: 2.81/2.92 N: 43.94/39.45	C: 25.8 ± 1.0 Zn: 9.7 ± 0.5 N: 41.9 ± 0.5 O: 22.6 ± 0.7	11.40
Pigment6	Magnesium titanium dioxide	TiMg_2O_4	-	Ti: 37.6 ± 2.1 Mg: 15.7 ± 0.8 O: 46.4 ± 1.3 Al: 0.3 ± 0.1	-
Pigment7	Magnesium iron oxide	MgFe_2O_4	-	Mg: 12.1 ± 1.1 Fe: 54.9 ± 3.5 O: 31.7 ± 2.3 Si: 1.1 ± 0.1 Al: 0.2 ± 0.1	-

The results of the SEM-EDS analysis of the studied pigments obtained at five different spots and averaged. The error bars represent the standard deviation from averaged values.

The following figures (Figures 7 and 8) show scanning electron micrographs of the prepared organic and inorganic pigments, where two images at two different magnifications are given for each pigment tested.

The SEM scans showed that the $\text{C}_6\text{H}_7\text{MgN}_9\text{O}_3$ and $\text{C}_{12}\text{H}_{16}\text{MgN}_{18}\text{O}_6$ pigments (Figure 7a–d) consisted of bulky sheet-like particles with less than 1 μm in diameter. In contrast, the particles of $\text{C}_{18}\text{H}_{26}\text{MgN}_{12}\text{O}_{14}$ and $\text{C}_{16}\text{H}_{18}\text{MgN}_{16}\text{O}_8$ pigments (Figure 7e–h) had an undefined polyhedral shape with wide size distribution. In the case of the $\text{C}_{12}\text{H}_{16}\text{ZnN}_{18}\text{O}_6$ pigment (Figure 7i,j), the undefined polyhedral particles can be identified as well, but their size distribution is significantly narrower and the diameter did not usually exceed 500 nm.

The particles of inorganic TiMg_2O_4 pigment (Figure 8a,b) were sintered into the larger agglomerates, with original spherical nature of primary particles still distinguishable. The slightly elongated primary particles of MgFe_2O pigment (Figure 8c,d) were sintered as well, but sharp needle-like structures can be identified in measured agglomerates. The TiO_2 pigment (Figure 8e,f) consisted of well-defined and separated small polyhedral nanoparticles with 50–200 nm in diameter.

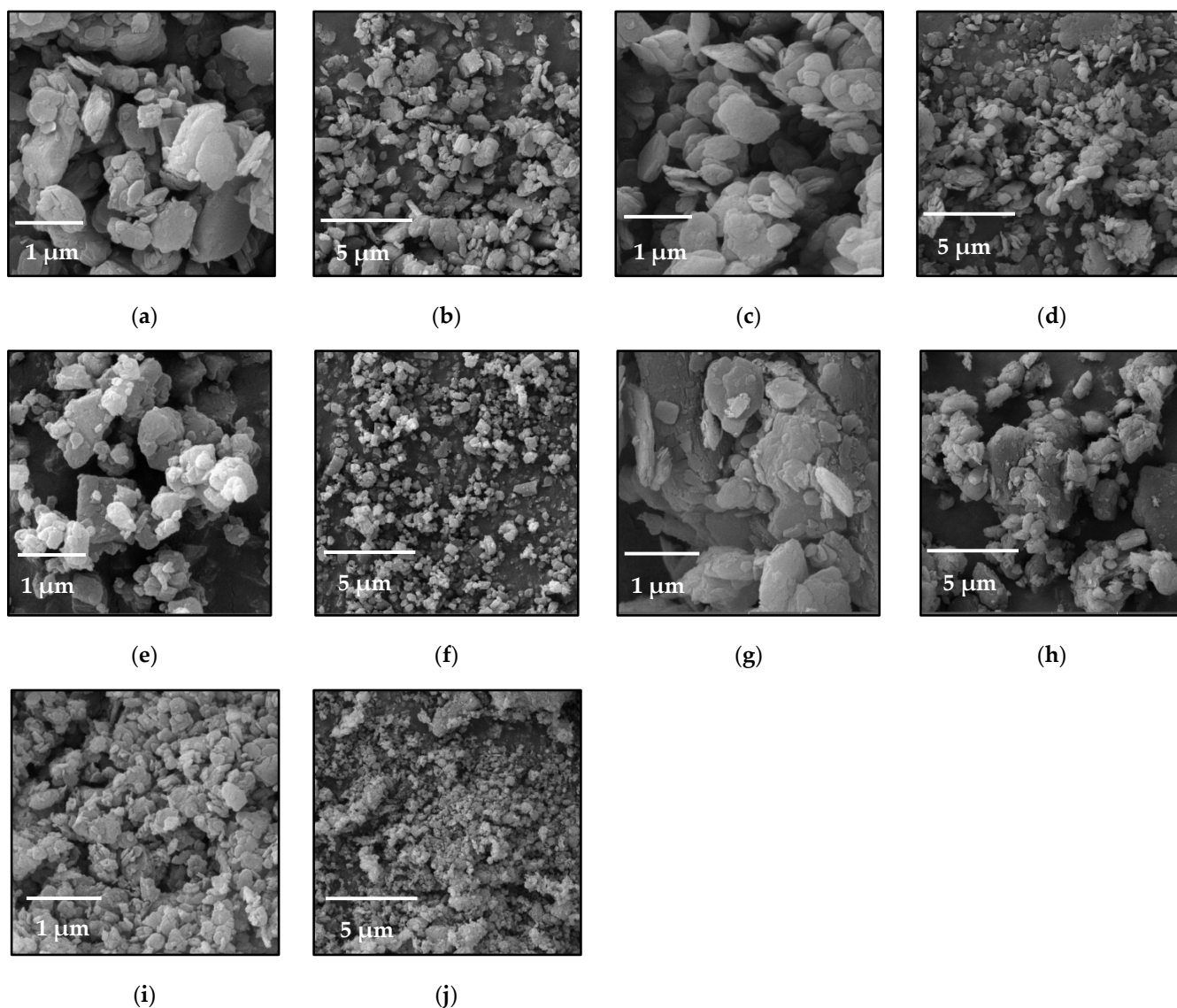


Figure 7. Scanning electron micrographs of the studied organic pigments: (a,b)— $\text{C}_6\text{H}_7\text{MgN}_9\text{O}_3$; (c,d)— $\text{C}_{12}\text{H}_{16}\text{MgN}_{18}\text{O}_6$; (e,f)— $\text{C}_{18}\text{H}_{26}\text{MgN}_{12}\text{O}_{14}$; (g,h)— $\text{C}_{16}\text{H}_{18}\text{MgN}_{16}\text{O}_8$; (i,j)— $\text{C}_{12}\text{H}_{16}\text{ZnN}_{18}\text{O}_6$.

These morphological properties of all tested pigments affect a number of properties of the films and can also affect the mechanical resistance of the film, adhesion, flexibility and many other properties [42,43].

The following figures (Figures 9 and 10) show the results of X-ray diffraction analysis of the studied organic and inorganic pigments. Individual organic pigments showed their intense characteristic peaks located at 2θ values. Pigment1 $\text{C}_6\text{H}_7\text{MgN}_9\text{O}_3$: 71.94, 68.14, 62.05, 58.61, 57.82, 50.81, 49.89, 39.74, 37.95, 33.23, 27.96, 28.44, 24.13, 21.96, 21.05, 18.53, 11.88, 10.92 and 10.62° . Pigment2 $\text{C}_{12}\text{H}_{16}\text{MgN}_{18}\text{O}_6$: 72.03, 68.23, 62.06, 58.62, 57.91, 50.78, 49.98, 37.95, 36.41, 33.21, 30.65, 28.03, 27.16, 23.95, 21.96, 19.81, 18.53, 11.85 and 10.89° . Pigment3 $\text{C}_{18}\text{H}_{26}\text{MgN}_{12}\text{O}_{14}$: 41.69, 41.06, 39.66, 37.01, 35.33, 33.58, 31.36, 30.04, 29.60, 28.93,

27.45, 26.40, 24.31, 22.02, 21.05, 20.52, 20.08, 19.63, 19.19, 18.44, 17.60, 16.90, 16.11, 15.44, 14.27, 13.87, 13.19, 12.84, 12.14, 9.78 and 8.77°. Pigment4 $C_{16}H_{18}MgN_{16}O_8$: 58.89, 50.95, 44.85, 40.54, 38.07, 36.83, 33.81, 33.14, 31.37, 29.20, 28.45, 26.69, 25.71, 23.06, 22.45, 21.49, 20.74, 19.91, 18.94, 18.58, 17.08, 16.06, 14.11, 13.29, 11.69 and 11.13°. Pigment5 $C_{12}H_{16}ZnN_{18}O_6$: 61.88, 48.39, 42.91, 43.63, 38.51, 33.49, 32.33, 30.65, 29.71, 27.94, 27.72, 25.71, 22.21, 21.04, 17.04, 13.02, 11.86, 10.91, 10.63 and 8.46°.

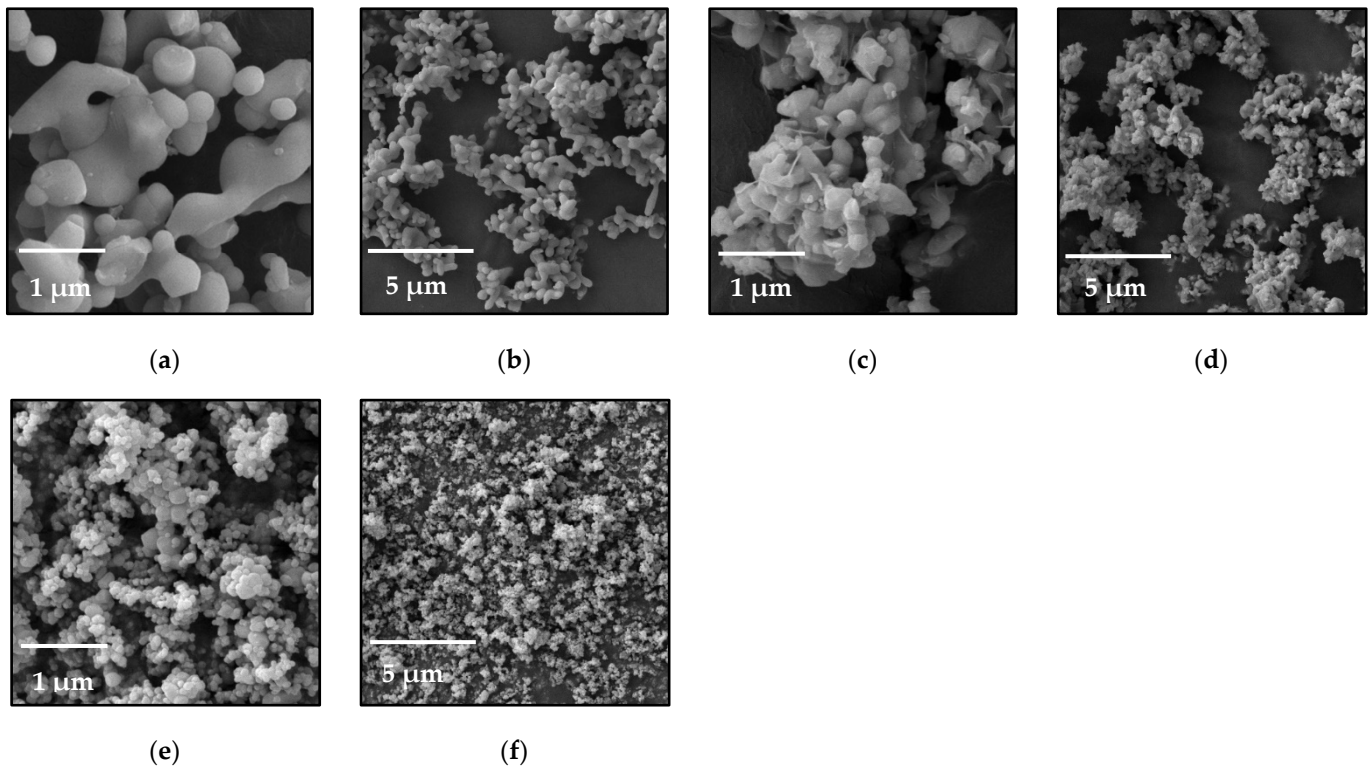


Figure 8. Scanning electron micrographs of the studied inorganic pigments: (a,b)— $TiMg_2O_4$; (c,d)— $MgFe_2O_4$; (e,f)— TiO_2 .

Inorganic pigments show a structure of mixed oxides. The main phase of the $TiMg_2O_4$ pigment is geikielite ($MgTiO_3$) and magnesium titanium oxide ($MgTi_2O_5$), and residues of unreacted starting materials such as rutile-type titanium dioxide and a small amount of unreacted magnesium oxide (MgO) were also found. A perovskite-type lattice was thus mainly formed with this pigment. This pigment is further still marked with the formula as $TiMg_2O_4$. The $MgFe_2O_4$ pigment consists mainly of magnesioferrite ($Mg(Fe^{3+})_2O_4$) and the remains of unreacted raw materials such as hematite (Fe_2O_3) and a small amount of unreacted magnesium oxide (MgO) were also found here. Therefore, a ferrite-type grid was mainly created. The content of MgO , which is relatively unreactive in pigments, is usually not a problem, as it has a positive effect on anti-corrosion efficiency [28]. This pigment is further labeled as $MgFe_2O_4$.

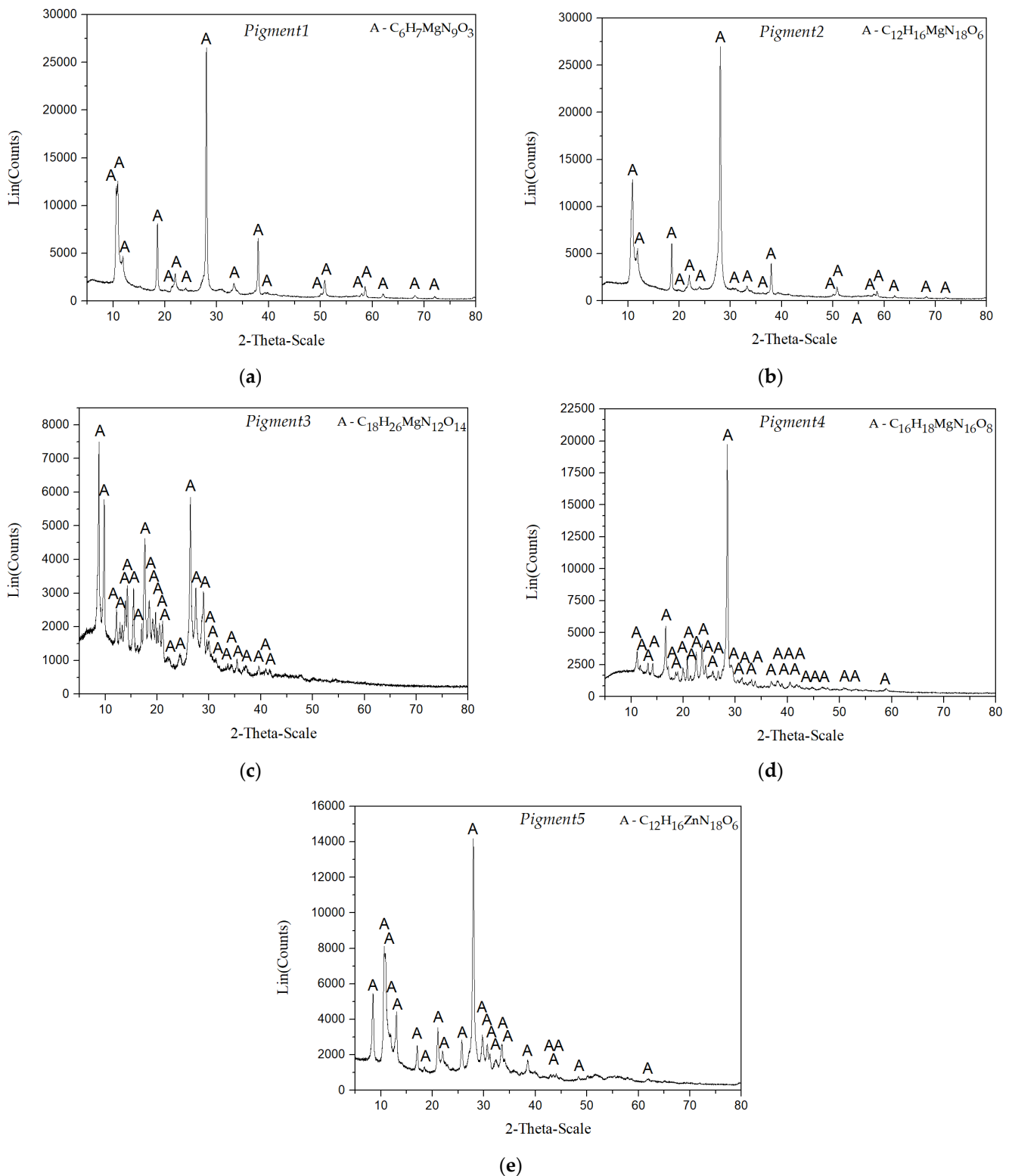


Figure 9. X-ray powder diffraction of the studied organic pigments: (a) $C_6H_7MgN_9O_3$; (b) $C_{12}H_{16}MgN_{18}O_6$; (c) $C_{18}H_{26}MgN_{12}O_{14}$; (d) $C_{16}H_{18}MgN_{16}O_8$; (e) $C_{12}H_{16}ZnN_{18}O_6$.

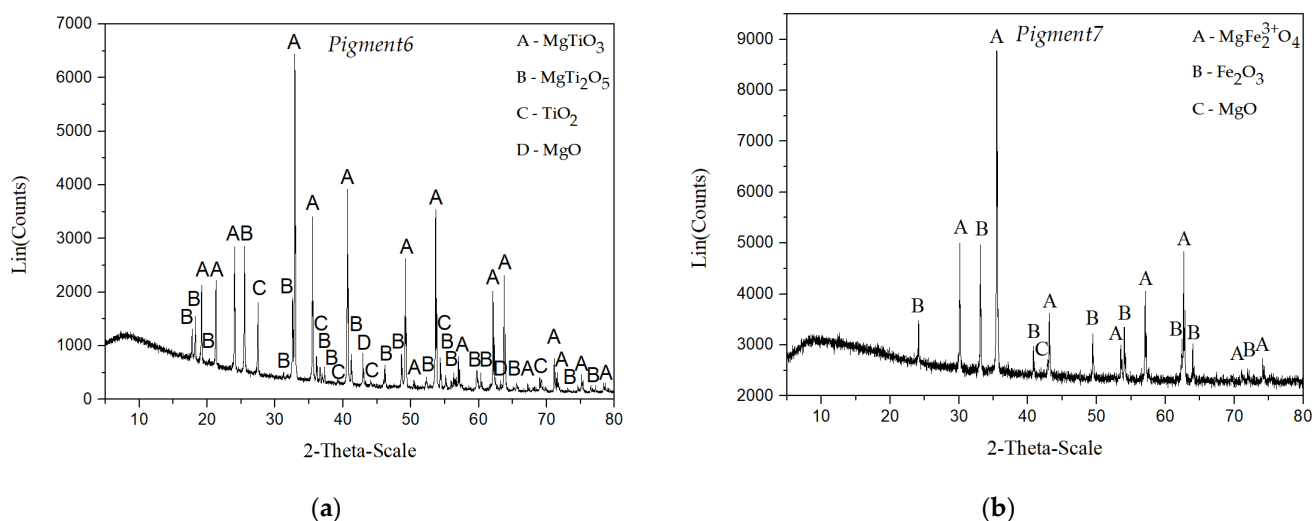


Figure 10. X-ray powder diffraction of the studied inorganic pigments: (a) TiMg_2O_4 ; (b) MgFe_2O_4 .

4.2. Physico-Chemical Properties of Powder Pigments

The values of densities, oil numbers and critical volume concentrations of individual pigments are shown in Table 3. The densities of the tested organic pigments ranged from $1.62 \pm 0.02 \text{ g}\cdot\text{cm}^{-3}$ ($\text{C}_{16}\text{H}_{18}\text{MgN}_{16}\text{O}_8$) to $1.92 \pm 0.02 \text{ g}\cdot\text{cm}^{-3}$ ($\text{C}_{12}\text{H}_{16}\text{MgN}_{18}\text{O}_6$). The densities of inorganic pigments ranged from $3.81 \pm 0.02 \text{ g}\cdot\text{cm}^{-3}$ (TiMg_2O_4) to $4.58 \pm 0.02 \text{ g}\cdot\text{cm}^{-3}$ (MgFe_2O_4). Oil absorption for organic pigments ranged from $30.02 \pm 0.2 \text{ g}/100 \text{ g}$ pigment ($\text{C}_6\text{H}_7\text{MgN}_9\text{O}_3$) to $36.42 \pm 0.2 \text{ g}/100 \text{ g}$ pigment ($\text{C}_{16}\text{H}_{18}\text{MgN}_{16}\text{O}_8$), which is due to the similarity in morphology and polydispersity of the particles of the tested pigments (Figure 7). The oil number values of the inorganic pigments reached lower values, which was caused by the different shape and size distribution of the particles (Figure 8). Oil number generally depends on the size and shape of the particles and the specific surface area and porosity of the pigment particles. Critical pigment volume concentration values have been calculated to range from approximately 57 to 70 for organic pigments and from 44 to 49 for inorganic pigments.

Table 3. Physico-chemical properties of the tested pigments.

Pigment	Oil Number [g/100 g Pigment]	Density [$\text{g}\cdot\text{cm}^{-3}$]	CPVC [–]
$\text{C}_6\text{H}_7\text{MgN}_9\text{O}_3$	30.02	1.75	64
$\text{C}_{12}\text{H}_{16}\text{MgN}_{18}\text{O}_6$	36.42	1.92	57
$\text{C}_{18}\text{H}_{26}\text{MgN}_{12}\text{O}_{14}$	31.25	1.72	70
$\text{C}_{16}\text{H}_{18}\text{MgN}_{16}\text{O}_8$	36.08	1.62	61
$\text{C}_{12}\text{H}_{16}\text{ZnN}_{18}\text{O}_6$	35.73	1.89	58
TiMg_2O_4	24.90	3.81	49
MgFe_2O_4	25.36	4.58	44
TiO_2	25.09	4.07	47
CaCO_3	22.55	2.71	60

Note: The parameter oil number and density are given as arithmetic averages within three measured values. Oil number was determined with an accuracy of $\pm 0.2 \text{ g}/100 \text{ g}$ pigment and density was determined with an accuracy of $\pm 0.02 \text{ g}\cdot\text{cm}^{-3}$.

4.3. Mechanical Properties of Pigmented Coatings Containing Studied Pigments

Organic coatings have been subjected to a series of mechanical tests providing information on their flexibility, strength, and adhesion. The results of these determinations for cases where comparable values were not achieved for all types of tested coatings are shown in Table 4. The measurement was carried out 60 days after the organic coating was applied to the substrate. Photographs of selected organic coatings after the pull of test are

shown in Figure 11. This figure shows the type of fracture in detail, specifically adhesion failure between substrate and first layer. This type of fracture was also noted when testing non-pigmented paint film.

Table 4. Mechanical properties of the tested coatings containing studied pigments.

Pigment	PVC [%]	Pull-Off Strength [MPa]	Relative Surface Hardness [%]
$C_6H_7MgN_9O_3$	0.10	4.2	44.3
	0.25	4.1	45.7
	0.50	4.5	47.9
$C_{12}H_{16}MgN_{18}O_6$	0.10	3.3	44.8
	0.25	3.8	45.6
	0.50	4.3	46.4
$C_{18}H_{26}MgN_{12}O_{14}$	0.10	3.8	42.9
	0.25	3.7	43.5
	0.50	3.0	43.7
$C_{16}H_{18}MgN_{16}O_8$	0.10	4.8	43.9
	0.25	4.6	44.5
	0.50	3.5	46.7
$C_{12}H_{16}ZnN_{18}O_6$	0.10	4.2	42.9
	0.25	4.9	43.7
	0.50	5.1	44.5
$TiMg_2O_4$	0.10	5.1	42.7
	0.25	4.6	43.3
	0.50	3.8	44.0
$MgFe_2O_4$	0.10	5.3	42.1
	0.25	4.3	43.3
	0.50	4.0	43.4
TiO_2	0.50	2.9	35.3

Note: The parameters are given as arithmetic averages within three measured values. Pull-off strength was determined with an accuracy of ± 0.2 MPa. The relative surface hardness was determined with an accuracy of $\pm 0.1\%$. The pull-off strength of the non-pigmented epoxy ester resin was 3.5 MPa.

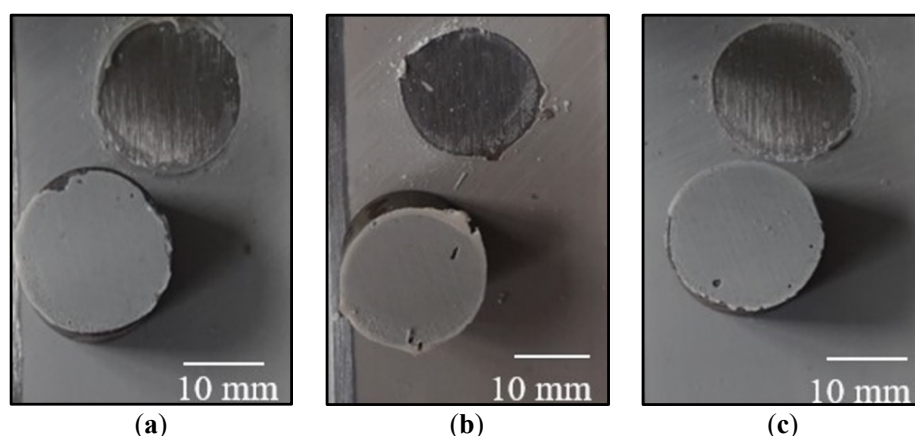


Figure 11. Determination of pull-off strength organic coatings at PVC = 0.50%: (a) with $C_{16}H_{18}MgN_{16}O_8$; (b) with $MgFe_2O_4$; (c) with TiO_2 .

When determining the resistance of organic coatings to bending deformation, the tested organic coatings showed high resistance, even when using a mandrel with the smallest diameter (4 mm). When determining the resistance of the organic coating to the cupping test, all tested organic coatings also showed high resistance, even with the maximum possible indentation of the steel ball (10 mm). Also, when determining the

resistance of the organic coating to a falling weight, no defects occurred when the weight was dropped from a maximum height of 100 cm. There were no defects in the tested organic coatings (when a weight was dropped from a height of 100 cm). When determining the adhesion of the individual organic coating on the steel substrate less than 5% of the total grid area was damaged (grade 1).

When the adhesion was determined by the pull-off test, the organic coating containing magnesium iron oxide MgFe_2O_4 showed the highest pull-off strength (5.3 MPa) at $\text{PVC} = 0.10\%$. Of the tested organic pigments, the pigment melamine orotate with magnesium cation $\text{C}_{16}\text{H}_{18}\text{MgN}_{16}\text{O}_8$ showed the greatest effect on adhesion at $\text{PVC} = 0.25\%$, for which the pull-off strength was determined to be 5.2 MPa. The measured values from the mechanical resistance tests did not change significantly with the increasing value of PVC, as the pigments were tested at relatively low values of PVC (0.10, 0.25 and 0.50%). It should be noted that the concentrations of the tested pigments were at a relatively low level; therefore, the binder itself contributed to the results, i.e., the epoxy ester resin, which has high adhesion to the metal surface due to OH groups [44]. For the organic coating containing only neutral titanium dioxide TiO_2 , a lower pull-off strength of 2.9 MPa was recorded. Thus, organic coatings containing synthesized organic and inorganic pigments have a positive effect on adhesion compared to a coating containing TiO_2 , which means that the newly synthesized pigments, with their morphology, especially the lamellar shape of the particles and surface properties, effectively ensure film adhesion and cohesion. The dominant fracture type noted in the evaluation of all coatings was adhesion failure between substrate and first layer (> 80%).

The surface hardness values of the coatings containing the synthesized tested pigments did not differ significantly; only the organic coating containing the neutral titanium dioxide had a lower relative surface hardness of 35.3% because this pigment (TiO_2) does not contain Mg or Zn cations, which have a positive effect on surface hardness. The relative surface hardness values increased with time for all coatings containing synthesized pigments approximately the same. The cations present in the pigments (Mg/Zn) at the chosen pigment volume concentration, therefore, had an effect on the speed of the oxypolymerization mechanism of the paint film drying (especially the Mg cation) [45]. The highest value of the relative surface hardness was achieved by the organic coating containing $\text{C}_6\text{H}_7\text{MgN}_9\text{O}_3$ at $\text{PVC} = 0.50\%$, i.e., 47.9%. At the same time, this pigment was found to have the highest magnesium content (from organic pigments). In addition, this pigment was characterized by regular lamellar particles. The reaction of carboxyl groups R-COOH and cations Mg^{2+} , or even Ca^{2+} and Zn^{2+} , produces carboxylates, so-called soaps, which increase the surface hardness of films and accelerate drying. These products, in the case of chemically active pigments, also have an effect on the corrosion resistance of coatings, as was studied, for example, in the case of aluminum. It should be noted that the surface hardness values of the coatings did not change significantly with the increasing value of PVC, as in the case of other mechanical tests. Based on the aforementioned mechanical properties of the tested organic coatings, the organic coatings containing synthesized organic and inorganic pigments show higher mechanical resistance and surface hardness than the organic coating containing neutral titanium dioxide. This is also a basic prerequisite for meeting the anti-corrosion properties of organic coatings [45,46].

4.4. Effect of Pigments on Corrosion Loss of Metal in an Aqueous Suspension of Powdered Pigments and Loose Paint Films

Results of the determination of relative corrosion losses ($X_{\text{rel-p}}$ and $X_{\text{rel-f}}$), pH values (pH_p and pH_f) and specific electrical conductivity (γ_p and γ_f) of aqueous pigment extracts and aqueous leaches of loose paint films at $\text{PVC}_{\text{pig}} = 0.50\%$ are shown in Table 5.

Table 5. Results of determination of relative corrosion losses pH values, and specific electrical conductivity.

Pigment	pH _p	γ _p [μS·cm ⁻¹]	X _{rel-p} [%]	pH _f	γ _f [μS·cm ⁻¹]	X _{rel-f} [%]
C ₆ H ₇ MgN ₉ O ₃	10.22	2713	28.47	4.47	105.7	17.86
C ₁₂ H ₁₆ MgN ₁₈ O ₆	10.06	1685	27.74	4.32	101.3	4.56
C ₁₈ H ₂₆ MgN ₁₂ O ₁₄	5.07	1624	43.07	4.01	104.2	72.02
C ₁₆ H ₁₈ MgN ₁₆ O ₈	8.83	4988	97.08	4.35	198.1	102.45
C ₁₂ H ₁₆ ZnN ₁₈ O ₆	7.82	1360	49.63	4.20	102.8	83.18
TiMg ₂ O ₄	10.71	1974	38.67	4.36	111.5	5.15
MgFe ₂ O ₄	10.65	1380	37.96	4.59	104.9	5.08
TiO ₂	7.53	1295	40.88	4.23	106.5	26.40

Note: Specific electrical conductivity was measured with an accuracy of $\pm 0.5 \mu\text{S}\cdot\text{cm}^{-1}$. The pH was measured with an accuracy of ± 0.01 . Values are given as arithmetic averages within three measured values. Values of pH and conductivity of redistilled water for the preparation of suspensions: pH = 6.85; $\gamma = 3.2 \mu\text{S}\cdot\text{cm}^{-1}$. Mass and relative corrosion loss of steel panels in redistilled water were $9.842 \text{ g}\cdot\text{cm}^{-2}$ and $X_p = 100\%$. The pH and conductivity of the unpigmented epoxy ester resin itself were pH = 5.55; $\gamma = 53 \mu\text{S}\cdot\text{cm}^{-1}$.

Low corrosion losses ($X_{\text{rel-p}}$) were measured for organic pigments based on cyanurate containing magnesium (C₆H₇MgN₉O₃ and C₁₂H₁₆MgN₁₈O₆) while inorganic pigments with Mg content showed slightly higher corrosion losses. In the case of these organic pigments, the influence of nitrogen on the aromatic ring, which suppressed the corrosion of the metal in the aqueous suspension, manifested itself in a favorable way [19,47]. The lowest $X_{\text{rel-p}}$ value was determined for the organic melamine cyanurate with magnesium cation C₁₂H₁₆MgN₁₈O₆, and that was 27.74% for the inorganic pigment MgFe₂O₄ the $X_{\text{rel-p}}$ value was equal to 37.96%. Conversely, the highest relative corrosion loss of $X_{\text{rel-p}}$ (97.08%) was measured in the aqueous leachate of the powder pigment melamine orotate with magnesium cation (C₁₆H₁₈MgN₁₆O₈), where the highest specific electrical conductivity was also found for this pigment. This means that with this pigment, there was excessive leaching of soluble components in the aqueous environment, which caused corrosion processes leading to the loss of the metal panel. These are probably the remains of unreacted starting substances, which are difficult to wash out during the pigment preparation process. These negative phenomena were also reflected in the results of the corrosion tests, as will be documented further.

Corrosion loss of pigmented films was also detected, which imitates the situation of placing coatings in an aqueous environment or during wetting, more precisely at the coating film/metal interface when wetting and in contact with water. The lowest relative corrosion loss of $X_{\text{rel-f}}$ was recorded for the aqueous leach of the film containing again melamine cyanurate with magnesium cation C₁₂H₁₆MgN₁₈O₆, namely 4.56%. Also, for the inorganic pigment MgFe₂O₄, a low relative corrosion loss was recorded, namely $X_{\text{rel-f}} = 5.08\%$. These two pigments also showed a significant effect on corrosion limitation in the case of laboratory corrosion tests, as will be documented below. The obtained data show that organic and inorganic pigments applied in the binder in the form of a pigmented coating have a significant inhibitory effect, as the values of corrosion losses from the aqueous leaching of aqueous leaches of loose paint films came close to each other. This means that the protective mechanism of the pigments in the paint film will be similar [14]. The positive effect of Mg cations in pigments on the reduction in corrosion losses is also documented by the example of leaching of a film containing a pigment without Mg content (titanium dioxide), where a higher relative corrosion loss $X_{\text{rel-f}} = 26.40\%$ was recorded. The highest relative corrosion loss ($X_{\text{rel-f}}$) was recorded for the aqueous leach of the film containing the organic pigment melamine orotate with magnesium cation C₁₆H₁₈MgN₁₆O₈, where the relative corrosion loss was 102%. The reason was a higher proportion of unreacted substances, as documented by its very high (highest) value of specific electrical conductivity. Therefore, this pigment also did not achieve the desired anti-corrosion performance even in the paint film when exposed to accelerated corrosion tests, as will be documented below.

Simultaneously with the measurement of corrosion losses ($X_{\text{rel-p}}$ and $X_{\text{rel-f}}$), the pH values (pH_p and pH_f) and the conductivity of powdered pigments and loose films were also determined. The highest pH_p values (10.71) of the aqueous extracts of pigments after measurement were shown by TiMg_2O_4 and also by the pigment MgFe_2O_4 ($\text{pH}_p = 10.65$), which is determined by the Mg content and structure of the pigment. It should be noted that this inorganic pigment TiMg_2O_4 contains a number of unreacted substances, which was confirmed by X-ray diffraction analysis (Figure 11a), which were further manifested in a negative influence both in the paint film and in the case of corrosion losses. The pH_p values of two organic pigments based on melamine cyanurate with magnesium cation reached similarly high values ($\text{pH}_p = 10.06$ and 10.22). Lower pH_p values (5.07) compared to other organic pigments were achieved by the aqueous leachate of the pigment melamine citrate with magnesium cation ($\text{C}_{16}\text{H}_{18}\text{MgN}_{16}\text{O}_8$), which is due to the structure of the pigment (lower Mg content) and the starting substance citric acid, which is a weak acid [48]. Relatively high values of electrical conductivity ($\gamma_p = 4998 \mu\text{S}\cdot\text{cm}^{-1}$) were achieved after 28 days by the aqueous leachate of the pigment melamine orotate with Mg cation ($\text{C}_{16}\text{H}_{18}\text{MgN}_{16}\text{O}_8$), which was probably caused by the remains of unreacted starting substances. This was also negatively reflected in the results of corrosion tests of pigmented paint films.

Measurements of pH and specific conductivity in conjunction with the determination of corrosion losses in both powder pigment suspension and paint film suspension document their importance in relation to the assessment of corrosion inhibition under the evaluated organic coatings, as will be documented further in the corrosion test results. The pH_p values of the pigments themselves and, at the same time, the specific conductivity γ_p have an effect on limiting corrosion, which, if it exceeds a certain value, has a negative effect on the protective inhibitory abilities of the pigments themselves and then on the pigmented paint films [14]. In paint films, in this case, these pH_f values are lower due to the character of the epoxy ester resin, but here too, the pH of the metal/film interface plays a role in limiting the rate of corrosion. If the pH of the paint film is increased due to pigments of an alkaline nature, this has a positive effect on slowing down and inhibiting corrosion processes under the organic coating [14].

4.5. Anti-Corrosion Efficiency of Pigmented Epoxy Ester Coatings in an Atmosphere Containing SO_2 and in an Atmosphere Containing Salt Electrolyte

Table 6 shows the results of the evaluation of the corrosion manifestations of the tested organic coatings after exposure to an atmosphere containing SO_2 and the pull-off strength after the corrosion test. A photograph of selected organic coating after 960 h exposure in atmosphere containing SO_2 and steel panels after removing the organic coating are shown in Figure 12. It can be seen from this Figure 12b,c that the presence of a blisters was recorded only in the close vicinity of the test cut, due to the penetration of the corrosive environment to the substrate through this defect, while the occurrence of a blisters was not recorded in the vicinity of the cut in Figure 12a. In addition, it can be seen from the pictures that the presence of red rust in the vicinity of the test cut was also noted for these two systems. Due to this fact, after the removal of the organic coating from the steel panel, the test cut was more significantly affected by corrosion in the systems where blistering around the cut was noted. This conclusion is shown in Figure 12d,e.

From the results shown in Table 6, it can be seen that no corrosion in the coating surface was noted for any of the organic coatings tested. In order to limit the degradation of the coating itself, it is also important to limit the formation of blisters on the surface of the coating films as low as possible. The most important characteristics for evaluating the anti-corrosion efficiency of coatings also include the effect on reducing corrosion of the metal substrate and the effect on reducing the spread of corrosion of the metal substrate in the section [23].

The highest effect on corrosion inhibition was shown by the organic coating containing $\text{C}_{12}\text{H}_{16}\text{MgN}_{18}\text{O}_6$ at PVC = 0.50%, where corrosion was recorded around the cut of 0.2 mm.

Additionally, no blistering around the cut was noted with this organic coating. An organic coating containing MgFe_2O_4 also showed higher corrosion resistance in an atmosphere containing SO_2 . This finding also means that there was no degradation of the metal surface.

After performing a corrosion test in an atmosphere containing SO_2 , the organic coating containing $\text{C}_{12}\text{H}_{16}\text{MgN}_{18}\text{O}_6$ at a PVC = 0.50% showed the highest pull-off strength, where a pull-off strength of 3.9 MPa was recorded. For the organic coating with this pigment, a trend was noted where the pull-off strength increased with increasing PVC. The organic one with MgFe_2O_4 also showed high pull-off strength (3.5 MPa). This finding also means that there was no degradation of the metal surface.

The organic coating containing TiO_2 showed the lowest pull-off strength after this corrosion test, at 0.5 MPa, which means that the penetrating corrosive SO_2 and water vapor degraded the barrier resistance of this coating. In the case of this organic coating, the occurrence of corrosion in the surface area of the substrate was 3%, and corrosion in the section was 2.6 mm, confirming that this pigment in the SO_2 atmosphere belongs to the neutral types of pigments, not to the types of inhibitory active and chemically acting types of corrosion inhibitors.

Table 6. Results of evaluation of corrosion resistance of organic coatings after 960 h of exposure in an atmosphere containing SO_2 . DFT = $100 \pm 10 \mu\text{m}$.

Pigment	PVC [%]	Blistering		Corrosion		Pull-Off Strength [MPa]
		On the Paint Surface [dg]	Near the Cut [dg]	Metal Base [%]	In the Cut [mm]	
$\text{C}_6\text{H}_7\text{MgN}_9\text{O}_3$	0.10	-	8MD	0.03	0.9	3.3
	0.25	8F	6D	16	1.6	1.7
	0.50	8F	8F	16	1.2	1.2
$\text{C}_{12}\text{H}_{16}\text{MgN}_{18}\text{O}_6$	0.10	-	8MD	1	1.9	2.6
	0.25	-	8MD	1	1.7	2.8
	0.50	-	-	0.03	0.2	3.9
$\text{C}_{18}\text{H}_{26}\text{MgN}_{12}\text{O}_{14}$	0.10	8F	6D	3	2.1	2.8
	0.25	8F	6D	1	2.2	2.7
	0.50	-	6D	1	1.4	3.3
$\text{C}_{16}\text{H}_{18}\text{MgN}_{16}\text{O}_8$	0.10	-	6D	1	1.4	3.4
	0.25	-	8D	1	1.4	3.5
	0.50	-	8D	3	1.8	2.6
$\text{C}_{12}\text{H}_{16}\text{ZnN}_{18}\text{O}_6$	0.10	8F	6D	3	2.0	2.1
	0.25	-	6D	1	2.1	2.2
	0.50	-	6D	0.3	2.1	3.0
TiMg_2O_4	0.10	-	8F	3	0.9	2.9
	0.25	8M	6MD	3	1.6	2.5
	0.50	8M	6D	3	2.1	2.4
MgFe_2O_4	0.10	-	6D	3	2.3	2.4
	0.25	-	6D	1	2.0	2.8
	0.50	-	8F	1	1.2	3.5
TiO_2	0.50	8F	8D	3	2.6	0.5

Note: The pull-off strength was determined with an accuracy of ± 0.2 MPa. The result is given as an arithmetic mean of three measured values. Corrosion parameters were determined on three test panels. The accuracy of measuring the distance of corrosion from the cut was ± 0.1 mm.

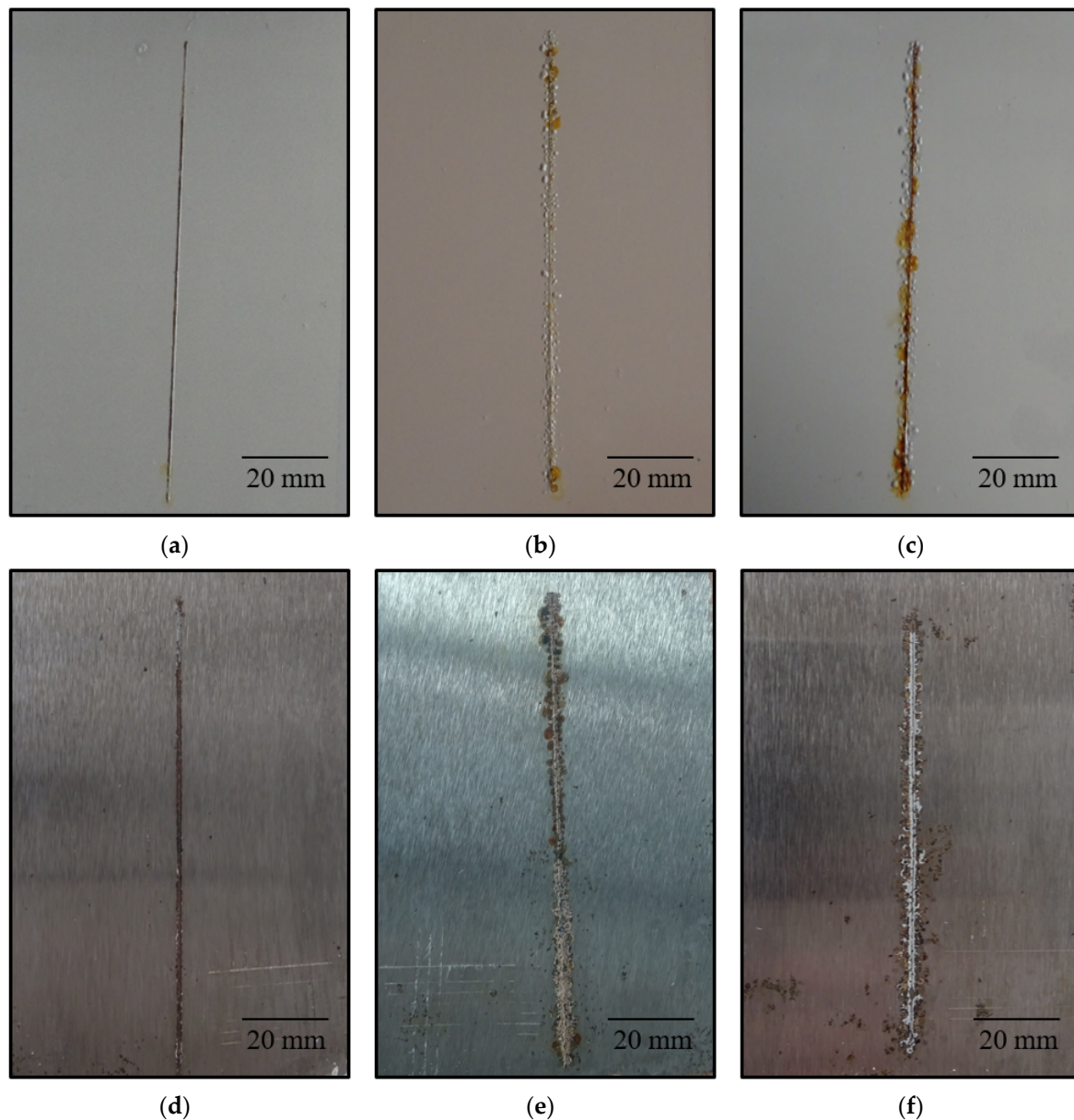


Figure 12. Organic coating after 960 h exposure in atmosphere containing SO_2 (a) with $\text{C}_{12}\text{H}_{16}\text{MgN}_{18}\text{O}_6$ at $\text{PVC} = 0.50\%$; (b) with MgFe_2O_4 at $\text{PVC} = 0.50\%$; (c) with TiO_2 ; and steel panel after removing the organic coating; (d) with $\text{C}_{12}\text{H}_{16}\text{MgN}_{18}\text{O}_6$ at $\text{PVC} = 0.50\%$; (e) with MgFe_2O_4 at $\text{PVC} = 0.50\%$; (f) with TiO_2 .

Table 7 shows the results of the evaluation of the corrosion manifestations of the tested organic coatings after exposure in an atmosphere containing salt electrolyte and the pull-off strength after the corrosion test. A photograph of selected organic coating after 960 h exposure in atmosphere containing salt electrolyte and steel panels after removing the organic coating is shown in Figure 13. It can be seen from this Figure 13a–c that the presence of blisters and the appearance of red rust near the test cut due to the penetration of chloride ions and other corrosion initiators to the steel substrate were noted for these organic coatings. Even with the organic coating shown in Figure 13c, blisters are evident in the panel surface, which were graded 8F. This fact also negatively affected the result of corrosion in the panel surface, which reached 3% for this coating, while this parameter reached a maximum value of 1% for the coating without the presence of blisters in the panel surface.

Table 7. Results of evaluation of corrosion resistance of organic coatings after 960 h of exposure in an atmosphere containing salt electrolyte. DFT = $100 \pm 10 \mu\text{m}$.

Pigment	PVC _{pig} [%]	Blistering		Corrosion		Pull-Off Strength [MPa]
		On the Paint Surface [dg]	Near the Cut [dg]	Metal Base [%]	In the Cut [mm]	
C ₆ H ₇ MgN ₉ O ₃	0.10	8M	8MD	1	1.6	3.2
	0.25	8M	8MD	3	2.3	3.8
	0.50	8M	6M	33	1.9	4.3
C ₁₂ H ₁₆ MgN ₁₈ O ₆	0.10	8F	2M	3	1.7	3.2
	0.25	8F	2F	1	1.6	3.7
	0.50	-	2F	1	1.4	3.8
C ₁₈ H ₂₆ MgN ₁₂ O ₁₄	0.10	8F	6M	3	1.5	2.8
	0.25	8F	6MD	3	1.7	3.6
	0.50	8F	6MD	3	1.8	3.8
C ₁₆ H ₁₈ MgN ₁₆ O ₈	0.10	8F	2M	1	1.8	4.4
	0.25	8M	2M	16	1.6	4.1
	0.50	8MD	6D	50	1.5	2.9
C ₁₂ H ₁₆ ZnN ₁₈ O ₆	0.10	8F	2F	1	1.6	2.7
	0.25	8F	2F	0.3	1.4	3.8
	0.50	-	8MD	0.1	1.3	4.5
TiMg ₂ O ₄	0.10	8F	4F	1	2.3	3.8
	0.25	8F	2MD	1	2.3	4.3
	0.50	8F	4M	1	2.0	3.3
MgFe ₂ O ₄	0.10	-	4F	0.1	1.8	4.3
	0.25	-	4F	1	1.8	4.3
	0.50	-	6F	1	1.7	4.1
TiO ₂	0.50	8F	2MD	3	2.4	1.4

Note: The pull-off strength was determined with an accuracy of ± 0.2 MPa. The result is given as an arithmetic mean of three measured values. Corrosion parameters were determined on three test panels. The accuracy of measuring the distance of corrosion from the cut was ± 0.1 mm.

From the results shown in Table 6, it can be seen that after completion of the accelerated corrosion test, no corrosion was noted in the surface of the coating, not even for one of the tested organic coatings. The most significant effect on corrosion inhibition, in this test, was also shown by an organic coating containing melamine cyanurate with Zn cations (C₁₂H₁₆ZnN₁₈O₆) at PVC = 0.50%, in which corrosion was recorded around the cut of 1.3 mm and occurrence of blisters on the surface of the coating was not recorded. In the case of exposure in an atmosphere containing salt fog, the influence of the Zn²⁺ cation in the structure of the complexing pigment was comparable to or even higher than in the case of the influence of the Mg²⁺ cation.

The highest occurrence of blisters in the area was recorded for the organic coating containing melamine orotate C₁₆H₁₈MgN₁₆O₈ at PVC = 0.50%, with a value of 6D, which was caused by the diffusion of water through the organic coating to the metal substrate and the subsequent release of soluble unreacted pigment substances, as was documented by an increase in specific electrical conductivity (Table 5). This process thus accelerated the corrosion of the metal substrate, led to a local loss of adhesion of the organic coating and the formation of blisters.

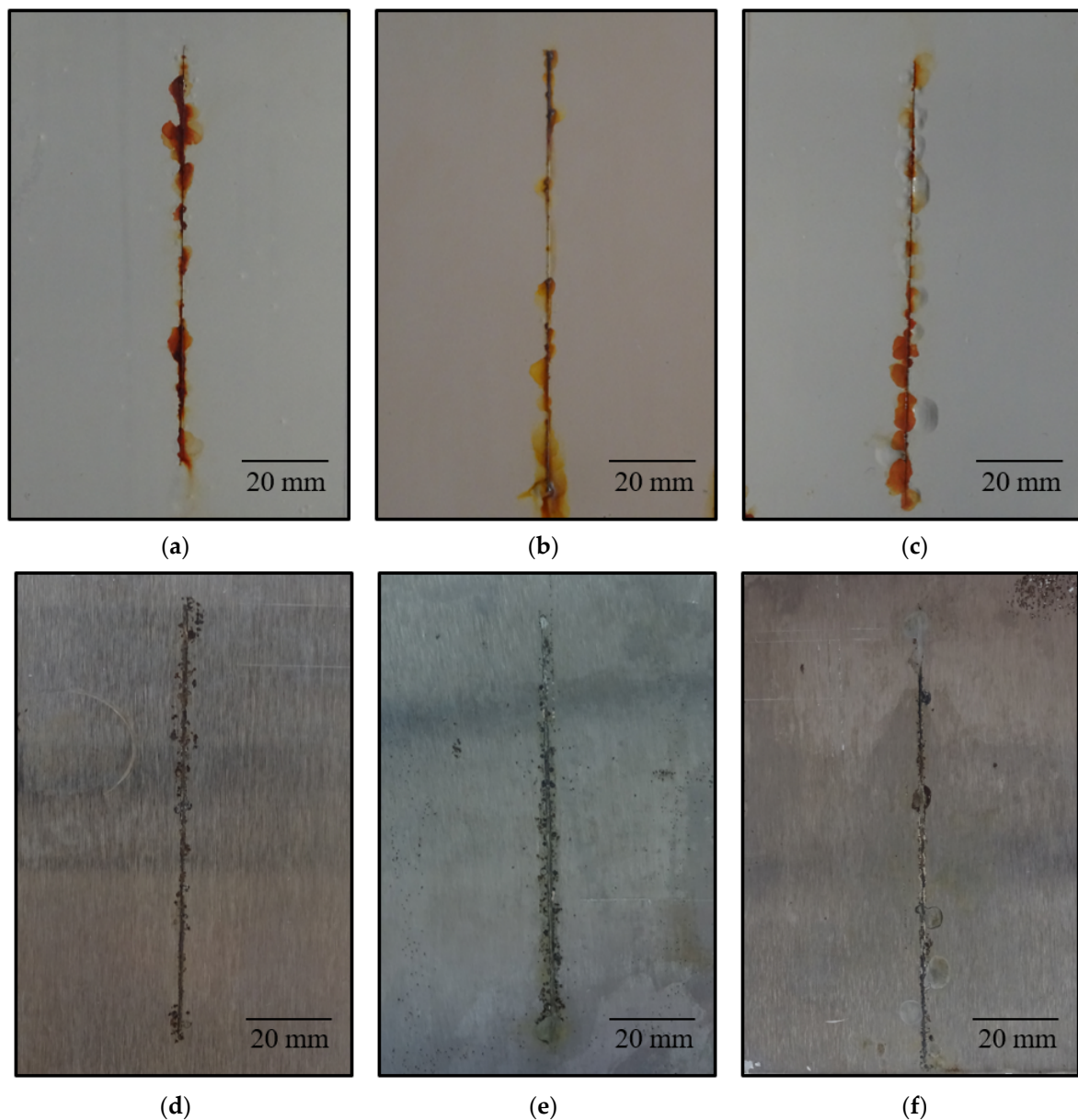


Figure 13. Organic coating after 960 h exposure in atmosphere containing salt electrolyte (a) with $C_{12}H_{16}MgN_{18}O_6$ at PVC = 0.50%; (b) with $MgFe_2O_4$ at PVC = 0.50%; (c) with TiO_2 ; and steel panel after removing the organic coating (d) with $C_{12}H_{16}MgN_{18}O_6$ at PVC = 0.50%; (e) with $MgFe_2O_4$ at PVC = 0.50%; (f) with TiO_2 .

After performing a corrosion test in an atmosphere containing a salt electrolyte, the organic coating containing $C_{12}H_{16}ZnN_{18}O_6$ at PVC = 0.50% showed the highest pull-off strength, where a pull-off strength of 4.5 MPa was recorded. For the organic coating with this pigment, a trend was noted where the pull-off strength increased with increasing PVC. High pull-off strength (4.2 MPa) was also shown by the organic material containing $MgFe_2O_4$ pigment. This finding also means that there was no degradation of the metal surface. The organic coating containing TiO_2 showed the lowest pull-off strength after this corrosion test was 1.4 MPa. This means that the lack of an active chemical corrosion inhibition mechanism and the barrier resistance of this coating were not sufficient to prevent the penetration of the corrosive salt electrolyte and water vapor.

4.6. Study of Anti-Corrosion Properties of Pigments Using the Electrochemical Method of Linear Polarisation

The results of the electrochemical techniques of linear polarization of the studied organic coatings after exposure in a 1 M NaCl solution are included in Table 8. Figure 14 shows Tafel plots of selected organic coatings containing the studied pigments, which are discussed below. These are the Tafel plots of organic coatings where the highest values of polarization resistance and the lowest values of corrosion rates were achieved.

Table 8. Results of linear polarization after exposure of the tested coatings in 1M NaCl solution, DFT = 50 ± 5 µm.

Pigment	PVC _{pig} [%]	E _{corr} [mV]	R _p [Ω]	Corrosion Rate [mm·Year ⁻¹]
C ₆ H ₇ MgN ₉ O ₃	0.10	−266	3.56 × 10 ⁶	2.57 × 10 ^{−5}
	0.25	−266	3.35 × 10 ⁶	2.75 × 10 ^{−5}
	0.50	−265	3.28 × 10 ⁶	2.77 × 10 ^{−5}
C ₁₂ H ₁₆ MgN ₁₈ O ₆	0.10	−319	4.81 × 10 ⁷	1.74 × 10 ^{−6}
	0.25	−318	5.36 × 10 ⁷	1.15 × 10 ^{−6}
	0.50	−285	4.28 × 10 ⁷	1.02 × 10 ^{−6}
C ₁₈ H ₂₆ MgN ₁₂ O ₁₄	0.10	−268	8.77 × 10 ⁵	1.05 × 10 ^{−4}
	0.25	−266	8.45 × 10 ⁵	1.09 × 10 ^{−4}
	0.50	−265	8.42 × 10 ⁵	1.09 × 10 ^{−4}
C ₁₆ H ₁₈ MgN ₁₆ O ₈	0.10	−262	5.01 × 10 ⁵	1.75 × 10 ^{−4}
	0.25	−260	3.03 × 10 ⁵	2.91 × 10 ^{−4}
	0.50	−258	2.87 × 10 ⁵	3.06 × 10 ^{−4}
C ₁₂ H ₁₆ ZnN ₁₈ O ₆	0.10	−286	3.24 × 10 ⁶	2.76 × 10 ^{−5}
	0.25	−285	3.22 × 10 ⁶	2.70 × 10 ^{−5}
	0.50	−282	3.29 × 10 ⁶	2.63 × 10 ^{−5}
TiMg ₂ O ₄	0.10	−268	7.78 × 10 ⁵	1.14 × 10 ^{−4}
	0.25	−266	7.99 × 10 ⁵	1.10 × 10 ^{−4}
	0.50	−262	8.29 × 10 ⁵	1.06 × 10 ^{−4}
MgFe ₂ O ₄	0.10	−298	4.45 × 10 ⁷	1.74 × 10 ^{−6}
	0.25	−301	4.49 × 10 ⁷	1.71 × 10 ^{−6}
	0.50	−305	4.95 × 10 ⁷	1.61 × 10 ^{−6}
TiO ₂	0.50	−192	2.48 × 10 ⁶	3.66 × 10 ^{−5}

Note: The results are given as an arithmetic mean of three measured values. The evaluated parameters were determined on three test panels. The polarization resistance of the non-pigmented epoxy ester resin film (DFT = 50 µm) was 6.50 × 10³ Ω, and corrosion rate of this film was 1.40 × 10^{−2} mm·year^{−1}.

The lowest value of the corrosion rate (1.61 × 10^{−6} mm·year^{−1}) and, at the same time, the highest value of the polarization resistance (4.95 × 10⁷ Ω) were recorded for the organic coating containing MgFe₂O₄ at PVC = 0.50%, a similar value of corrosion rate (1.02 × 10^{−6} mm·year^{−1}) and a lower value of polarization resistance (4.28 × 10⁷ Ω) were recorded for the organic coating containing C₁₂H₁₆MgN₁₈O₆ at PVC = 0.50%. For both mentioned pigments, the dependence of PVC on the corrosion rate was recorded, whereas when the PVC value increased, the corrosion rate values decreased. Organic coatings containing the pigment C₁₂H₁₆ZnN₁₈O₆ achieved an order of magnitude lower polarization resistance and an order of magnitude higher corrosion rate compared to the above-mentioned most effective organic coatings. For the organic coating containing TiO₂, a corrosion rate of 3.66 × 10^{−5} mm·year^{−1} and a polarization resistance of 2.48 × 10⁶ Ω were recorded. This means that the neutral TiO₂ pigment exhibits a barrier mechanism in the coating film. Pigments MgFe₂O₄ and C₁₂H₁₆MgN₁₈O₆ also show a chemical mechanism of protective action in the paint film, therefore, their corrosion characteristics are more favorable. The protective properties of these pigments have also

been proven using laboratory tests in corrosive atmospheres. It should be noted that the concentration in the paint film was very low (0.10–0.50%), i.e., 10- or up to 20-fold lower than is usual for classic anti-corrosion pigments. Such dosage values in paint materials usually have corrosion inhibitors, which are added to classic anti-corrosion pigments [49].

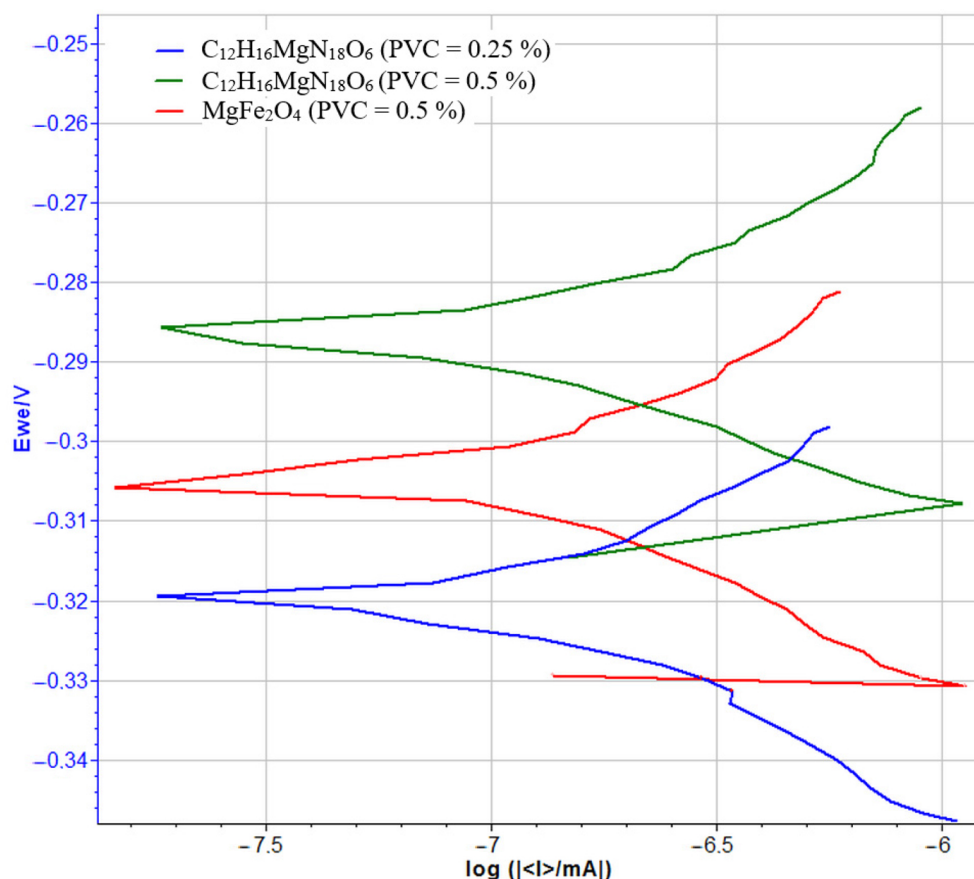


Figure 14. Tafel plots of the studied organic coatings containing: $C_{12}H_{16}MgN_{18}O_6$ (PVC = 0.25%), $C_{12}H_{16}MgN_{18}O_6$ (PVC = 0.50%), and $MgFe_2O_4$ (PVC = 0.50%).

4.7. Corrosion Inhibition Mechanism of Action of Pigments in the Paint Film

In this study, the anti-corrosion performance of synthesized organic and inorganic pigments in paint films was evaluated. The organic pigment melamine cyanurate with magnesium cation ($C_{12}H_{16}MgN_{18}O_6$) and the inorganic pigment magnesium ferrous ($MgFe_2O_4$), which contained sufficient Mg^{2+} to provide a complex protective mechanism in the paint film at relatively low concentration (PVC), achieved the highest anti-corrosion performance and also the best properties.

The organic pigment melamine cyanurate with magnesium cation ($C_{12}H_{16}MgN_{18}O_6$) showed the highest resistance when tested in an atmosphere containing SO_2 at PVC = 0.50%, where blisters were not recorded in the test cut when evaluating corrosion on the surface of the substrate, value was recorded 0.03%, and in the test cut, the corrosion reached the value of 0.2 mm. During the test in an atmosphere containing a salt electrolyte, blisters were recorded on the organic coating with this pigment on the paint film surface 8F, in the test cut 2F, in the evaluation of the corrosion on the surface of the steel substrate, a corrosion value of 1% was recorded. In the test cut, the corrosion reached a value of 1.4 mm. The protective capabilities of this pigment were also confirmed by the electrochemical technique of linear polarization, where it was recorded a corrosion rate of $1.02 \times 10^{-6} \text{ mm} \cdot \text{year}^{-1}$ (the lowest recorded corrosion rate of all tested organic pigments). This result also confirmed the overall high anti-corrosion efficiency of the organic coating pigmented this organic

pigment. In the aqueous leachate of this pigment, a weight corrosion loss of $1.895 \text{ g}\cdot\text{m}^{-2}$ and a relative weight corrosion loss of 27.74% were recorded, which is the smallest corrosion loss of all the tested pigments. In the aqueous leach of the loose film of this pigment, a weight corrosion loss of $0.449 \text{ g}\cdot\text{m}^{-2}$ and a relative weight corrosion loss of 4.56% was recorded, which is again the smallest corrosion loss of all the tested pigments.

The inorganic pigment magnesium iron oxide (MgFe_2O_4), when determining corrosion resistance in an atmosphere containing SO_2 , showed high resistance even at $\text{PVC} = 0.50\%$, where no blisters were recorded on the paint film surface, blisters around the cut reached a value of 8F when evaluating the corrosion on the area of the steel base, a corrosion value of 1% was recorded, and in the section, the corrosion reached a value of 1.2 mm. When determining the corrosion resistance in an atmosphere containing a salt electrolyte, the organic coating showed the highest resistance at $\text{PVC} = 0.1\%$, where no blisters were found on the paint film area, and blisters around the cut reached the value of 4F. When evaluating the corrosion on the surface of the steel substrate, a corrosion value of 0.1 was recorded %, and in the test cut, the corrosion reached a value of 1.8 mm. After performing the linear polarization electrochemical technique, a corrosion rate of $1.61 \times 10^{-6} \text{ mm}\cdot\text{year}^{-1}$ was recorded for this coating at $\text{PVC} = 0.50\%$, which was the lowest corrosion rate recorded for the tested organic coatings containing inorganic pigments. In the aqueous leachate of this pigment, a weight corrosion loss of $2.643 \text{ g}\cdot\text{m}^{-2}$ and a relative weight corrosion loss of 37.96% were recorded. In the aqueous leach of the loose film of this pigment, a weight corrosion loss of $0.499 \text{ g}\cdot\text{m}^{-2}$ and a relative weight corrosion loss of 5.08% were recorded, which is almost the lowest corrosion loss among the tested pigments.

Both of these pigments ($\text{C}_{12}\text{H}_{16}\text{MgN}_{18}\text{O}_6$ and MgFe_2O_4) contain Mg^{2+} cations in their structure, which have a beneficial effect on reducing the corrosion of the metal substrate and the corrosion rate due to the effect of increasing the pH values around the surface of the metal substrate. Measurement of corrosion losses shows a positive effect of Mg on the properties of both the powder pigment and the pigmented film, where the protective effect is maximal for these pigments with a high Mg^{2+} content. The chemical action as an important part of the protective action of these two pigments is also strengthened due to the fact that in the epoxy ester film, the Mg^{2+} cations of organic and inorganic pigments form salts–soap (Mg carboxylates) by reaction with the carboxyl groups of this binder.

The barrier mechanism of protection is intrinsic to every properly formulated coating. Significant effect on adhesion barrier capabilities, or to strengthen them, they have a suitable part shape, especially lamellar [42]. Some of the tested pigments proved this, as can be seen from the SEM and, at the same time, from the values from the adhesion tests. In addition to the carboxyl R-COOH groups, the epoxy ester resin itself also has OH groups, which increase the adhesion of this type of coating. Thanks to the presence of the tested pigments and the formation of Mg carboxylates, there was also an increase in the mechanical resistance of the coatings, as documented by the relevant results. However, such a phenomenon did not occur with a coating with an inert pigment, without a lamellar shape of particles, and without Mg cation content. Faster drying of the film and higher surface hardness of the film due to the presence of organic pigments with Mg/Zn content, as can be seen from the relevant measurements, also means higher mechanical resistance of the given organic coating and the possibility of its rapid loading during application in practice. The excellent adhesion barrier properties of the binder based on esterified epoxy resin strengthen the tested organic pigments thanks to the NH_2 groups in the structure, which can act during the life of the paint film and extend its life when exposed to corrosive influences.

OH^- ions are formed at the corrosion cathodic sites, so a protective film of $\text{Mg}(\text{OH})_2$ on the surface is ensured both in the case of organic and inorganic tested pigments. The values of polarization resistance are relatively high for coatings containing these pigments, even at such a low concentration of PVC. Compared to the original non-pigmented resin or coating with TiO_2 , they show up to 10- and even 10,000-fold higher values. In the case of an organic pigment, which, due to its structure, has the ability to bind Fe^{2+} corrosion products into a complex in the area of anodic sites, it is possible to apply this mechanism

in the case when the surface of the pigment is in contact with the steel surface (see X_{rel-p} values). In the case of organic pigments, the active action of a large molecule with N_2 is also important, by which it binds to the anodic sites of the metal surface. Figure 15 clearly documents the individual parts of the protective action in the paint film.

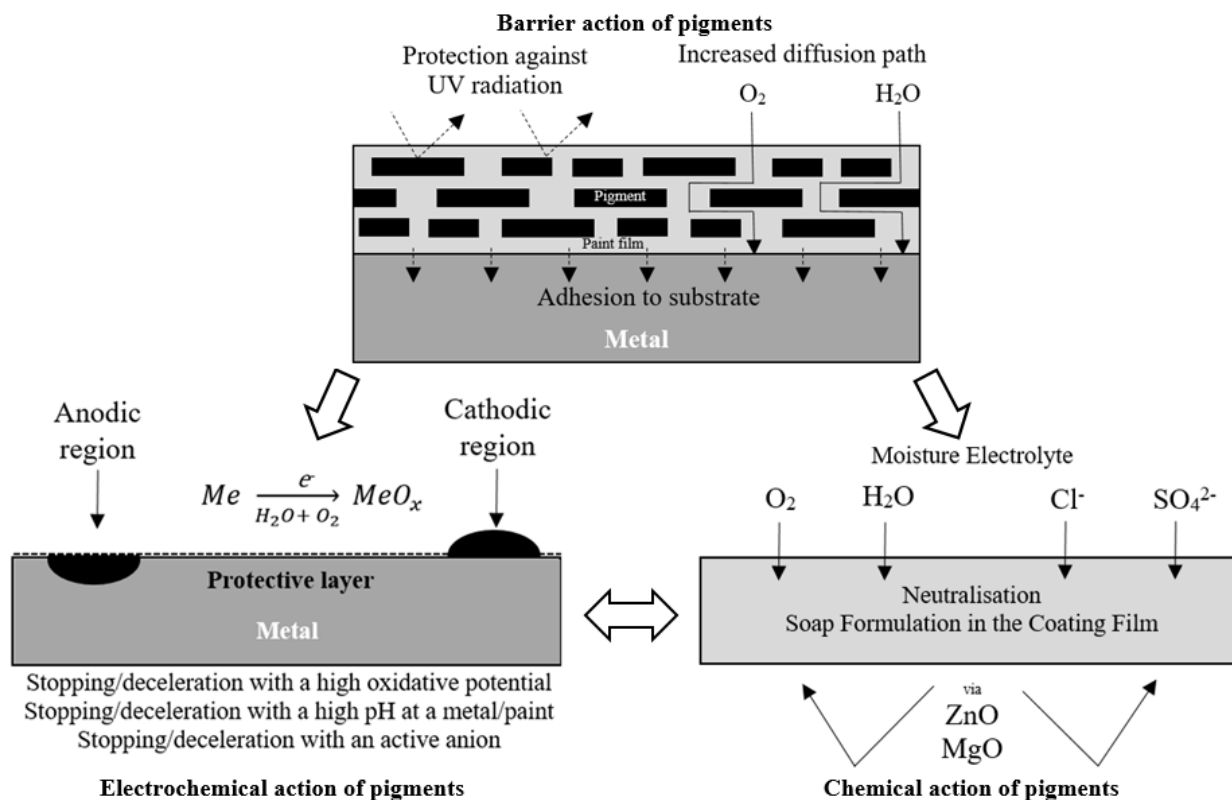


Figure 15. Chemical, electrochemical, and barrier action (mechanism) of pigments in a paint film [34,35,50].

5. Conclusions

This article deals with preparation and testing of pigments based on melamine cyanurate with Mg^{2+} or Zn^{2+} , melamine citrate with Mg^{2+} and melamine orotate with Mg^{2+} in the form of a complex. As comparative pigments, inorganic pigments magnesium titanium dioxide and magnesium iron oxide were synthesized using high-temperature synthesis. The effect of pigments on corrosion and mechanical resistance was tested in a paint based on epoxy-ester resin at three different concentrations. The anti-corrosion efficiency of pigmented organic coatings was determined using laboratory corrosion tests in the environment of a salt electrolyte, in an atmosphere containing SO_2 and using the linear polarization electrochemical method. The results of corrosion tests of organic pigments based on melamine differed mainly depending on the type of additional structural component, i.e., the presence of a structural unit of cyanurate, citrate, or orotate. Based on the results cyclic corrosion tests, one type of organic pigment melamine cyanurate with the magnesium cation ($C_{12}H_{16}MgN_{18}O_6$) was selected, which achieved a similar anti-corrosion efficiency compared to the inorganic pigment ($MgFe_2O_4$). Where both types of pigments were used, the corrosion resistance of the coatings increased with increasing PVC value. Coatings pigmented with these pigments had a significant effect on corrosion resistance in an acidic atmosphere containing SO_2 and in an atmosphere containing a salt electrolyte. This conclusion was also confirmed by the results of the electrochemical technique of linear polarization, when these two types of pigments (with three values of PVC) achieved at least one order of magnitude higher polarization resistance compared to the other types of pigments studied. Based on the results of the corrosion test in an atmosphere containing

salt spray, the above-mentioned two types of organic coatings (at PVC = 0.50%) with the highest anti-corrosion efficiency can be recommended for the C3 corrosion environment (corresponds to dry climates), according to EN ISO 12944. Further based on the results of mechanical tests, it can be concluded that the studied organic coatings with the highest anti-corrosion efficiency (organic coating containing melamine cyanurate with the magnesium cation at PVC = 0.50% and organic coating containing magnesium iron oxide at PVC = 0.50%) can be recommended for the protection of steel structures that will be mechanically stressed, as their mechanical resistance after the relevant (ISO) tests reached maximum values and tear strength values higher than 4 MPa.

Author Contributions: Conceptualization, M.K., F.A., R.H. and A.K. (Andréa Kalendová); methodology, M.K., F.A., A.K. (Anna Krejčová), S.S. and D.Ř.; software, M.K.; validation, M.K. and A.K. (Andréa Kalendová); formal analysis, M.K., K.B., A.K. (Anna Krejčová) and S.S.; investigation, M.K.; resources, M.K. and D.Ř.; data curation, M.K. and D.Ř.; writing—original draft, M.K., F.A., K.B., D.Ř., R.H. and A.K. (Andréa Kalendová); writing—review and editing, M.K., F.A., K.B., R.H. and A.K. (Andréa Kalendová); visualization, M.K., R.H. and A.K. (Andréa Kalendová); supervision, R.H. and A.K. (Andréa Kalendová). All authors have read and agreed to the published version of the manuscript.

Funding: Authors appreciate financial support from grant FV30048, FV-TRIO (2016–2021), The Ministry of Industry and Trade, Czech Republic, GAMA2-01/002, TG302102 Technology Agency of the Czech Republic, and LM2023037 from the Ministry of Education, Youth and Sports of the Czech Republic.

Institutional Review Board Statement: Not applicable.

Informed Consent Statement: Not applicable.

Data Availability Statement: Data sharing is not applicable to this article.

Conflicts of Interest: The authors declare no conflict of interest.

References

1. Ziganshina, M.; Stepin, S.; Karandashov, S.; Mendelson, V. Complex oxides—Non-toxic pigments for anticorrosive coatings. *Anti-Corros. Methods Mater.* **2020**, *67*, 395–405. [[CrossRef](#)]
2. Al Jahdaly, B.A.; Maghraby, Y.R.; Ibrahim, A.H.; Shouier, K.R.; Alturki, A.M.; El-Shabasy, R.M. Role of green chemistry in sustainable corrosion inhibition: A review on recent developments. *Mater. Today Sustain.* **2022**, *20*, 100242. [[CrossRef](#)]
3. Sharma, S.; Kumar, A. Recent advances in metallic corrosion inhibition: A review. *J. Mol. Liq.* **2021**, *322*, 114862. [[CrossRef](#)]
4. Umoren, S.A.; Solomon, M.M. Synergistic corrosion inhibition effect of metal cations and mixtures of organic compounds: A Review. *J. Environ. Chem. Eng.* **2017**, *5*, 246–273. [[CrossRef](#)]
5. Akpan, E.D.; Singh, A.K.; Lgaz, H.; Quadri, T.W.; Shukla, S.K.; Mangla, B.; Dwivedi, A.; Dagdag, O.; Sheetal Inyang, E.E.; Ebenso, E.E. Coordination compounds as corrosion inhibitors of metals: A review. *Coord. Chem. Rev.* **2024**, *499*, 215503. [[CrossRef](#)]
6. Hajjari, A.; Shahrabi, T.; Mohammadi, I. Synthesis of a novel environmentally friendly hybrid pigment for effective corrosion control of mild steel. *J. Environ. Chem. Eng.* **2023**, *11*, 109383. [[CrossRef](#)]
7. Molina, J.; Puig, M.; Gimeno, M.J.; Izquaiardo, R.; Gracenea, J.J.; Suay, J.J. Influence of zinc molybdenum phosphate pigment on coatings performance studied by electrochemical methods. *Prog. Org. Coat.* **2016**, *97*, 244–253. [[CrossRef](#)]
8. Sorensen, P.A.; Kill, S.; Dam-Johansen, K.; Weinell, C.E. Anticorrosive coatings: A review. *J. Coat. Technol. Res.* **2009**, *6*, 135–176. [[CrossRef](#)]
9. Yong, Z.; Qiu, C.; Liu, Y. Molybdate/phosphate composite conversion coating on magnesium alloy surface for corrosion protection. *Appl. Surf. Sci.* **2008**, *255*, 1672–1680. [[CrossRef](#)]
10. Yang, J.; Li, Z.; Shi, J.; Yan, Z. Study on the corrosion inhibition performance of sodium silicate and polyaspartic acid for 35CrMo steel. *Int. J. Electrochem. Sci.* **2023**, *18*, 100042. [[CrossRef](#)]
11. Balaskas, A.C.; Kartsonakis, I.A.; Snihirova, D.; Montemor, M.F.; Kordas, G. Improving the corrosion protection properties of organically modified silicate–epoxy coatings by incorporation of organic and inorganic inhibitors. *Prog. Org. Coat.* **2011**, *72*, 653–662. [[CrossRef](#)]
12. Govindaraj, Y.; Venkatachalam, D.; Prabhakar, M.; Manikandanath, N.T.; Balaraju, J.N.; Rohwerder, M.; Neelakantan, L. Nano-sized cerium vanadium oxide as corrosion inhibitor: A microstructural and release study. *Electrochim. Acta* **2022**, *425*, 140696. [[CrossRef](#)]

13. Kumar, H.; Sharma, R.; Yadav, A.; Kumari, R. Synthesis, characterization and influence of reduced Graphene Oxide (rGO) on the performance of mixed metal oxide nano-composite as optoelectronic material and corrosion inhibitor. *Chem. Data Collect.* **2020**, *29*, 100527. [[CrossRef](#)]
14. Brodinová, J.; Stejskal, J.; Kalendová, A. Investigation of ferrites properties with polyaniline layer in anticorrosive coatings. *J. Phys. Chem. Solids* **2007**, *68*, 1091–1095. [[CrossRef](#)]
15. Lin, S.; Zhang, T. Research progress in preparation and application of spinel-type metallic oxides ($M \geq 2$). *J. Alloys Compd.* **2023**, *962*, 171117. [[CrossRef](#)]
16. Salih, S.J.; Mahmood, W.M. Review on magnetic spinel ferrite (MFe_2O_4) nanoparticles: From synthesis to application. *Heliyon* **2023**, *9*, e16601. [[CrossRef](#)] [[PubMed](#)]
17. Mahmoodi, A.; Jiryaei, Z.; Dadras, A.; Khorasani, M.; Shi, X. A hybrid yellow nano pigment as an environmentally sound alternative to lead chromate pigment for pavement markings. *J. Clean. Prod.* **2021**, *319*, 128733. [[CrossRef](#)]
18. Wang, C.; Peng, Y.; Fu, S.; Yang, X.; Ne, C.; Wang, X.; Cang, G.; Liang, Z.; Li, J. Experimental and theoretical investigations of 1,1'-Dibenzyl-[4,4'-bipyridine]-1,1'-dium chloride as effective corrosion inhibitor for Q235 steel in 1 M HCl. *Mater. Today Commun.* **2023**, *35*, 106169. [[CrossRef](#)]
19. Zhu, H.; Liu, J.; Lu, X.; Wang, D.; Geng, T.; Feng, L.; Liang, D.; Ma, X.; Chu, C. Wettability and anticorrosion behavior of organic-inorganic hybrid superhydrophobic epoxy coatings containing triazine corrosion inhibitor loaded in the mesoporous molecular sieve. *J. Taiwan Inst. Chem. Eng.* **2022**, *141*, 104604. [[CrossRef](#)]
20. Zhang, Z.; Yan, D.; Liu, X.; Li, W.; Wang, Z.; Wang, Y.; Song, D.; Zhang, T.; Liu, J.; Wang, J. Self-healing nanocomposite coatings containing organic-inorganic inhibitors functionalized dendritic silica nanocontainers for synergistic corrosion protection of carbon steel. *Colloids Surf. A Physicochem. Eng. Asp.* **2023**, *656*, 130430. [[CrossRef](#)]
21. Freitas, B.R.; Braga, J.O.; Orlandi, M.P.; Da Silva, B.P.; Aoki, I.V.; Lins, V.F.C.; Cotting, F. Characterization of coir fiber powder (cocos nucifera L.) as an environmentally friendly inhibitor pigment for organic coatings. *J. Mater. Res. Technol.* **2022**, *19*, 1332–1342. [[CrossRef](#)]
22. Sahin, N.; Kula, I.; Erdogan, Y. Investigation of antimicrobial activities of nonanoic acid derivatives. *Fresenius Environ. Bull.* **2006**, *15*, 141–143.
23. Zhao, X.; Qi, Y.; Zhang, Z.; Li, K. The Influence of Glass Flake and Micaceous Iron Oxide on Electrochemical Corrosion Performance of Waterborne Silicate Coatings in 3.5% NaCl Solution. *Coatings* **2019**, *9*, 833. [[CrossRef](#)]
24. Hrdina, R.; Burgert, L.; Kalendová, A.; Alafid, F.; Panák, A.; Držková, O.; Kohl, M. Use of Salts of Perylenic Acid as Anticorrosive Substances. Czech Republic No. 308991. 29 September 2021.
25. Marzec, A.; Szadkowski, B.; Rogowski, J.; Maniukiewicz, W.; Rybinski, P.; Prochon, M. New Organic/Inorganic Pigments Based on Azo Dye and Aluminum-Magnesium Hydroxycarbonates with Various Mg/Al Ratios. *Materials* **2019**, *12*, 1349. [[CrossRef](#)] [[PubMed](#)]
26. Suzuki, E.M. Infrared spectra of North American automobile original finishes XI: In situ identification of perylene pigments—Analysis of Perylene Maroon (C.I. Pigment Red 179) and alumina-based red pearlescent pigments. *Forensic Chem.* **2021**, *25*, 100351. [[CrossRef](#)]
27. Xue, Y.-N.; Xue, X.-Z.; Miao, M.; Liu, J.-K. Mass preparation and anticorrosion mechanism of highly triple-effective corrosion inhibition performance for co-modified zinc phosphate-based pigments. *Dye. Pigment.* **2019**, *161*, 489–499. [[CrossRef](#)]
28. Plagemann, P.; Weise, J.; Zockoll, A. Zinc-magnesium-pigment rich coatings for corrosion protection of aluminum alloys. *Prog. Org. Coat.* **2013**, *76*, 616–625. [[CrossRef](#)]
29. Perdigão, L.; Champness, N.; Beton, P. Surface self-assembly of the cyanuric acid–melamine hydrogen bonded network. *Chem. Commun.* **2006**, *5*, 538–540. [[CrossRef](#)]
30. Li, Z.; Wang, X.; Tan, Y.; Qu, B. Synergistic effects and flame-retardant properties of melamine cyanurate with magnesium hydroxide in halogen-free flame-retardant EVA blends. *Fire Sci. Technol.* **2005**, *24*, 320–326.
31. Liu, Y.; Wang, Q. The investigation of melamine cyanurate encapsulating magnesium hydroxide flame retarded polyamide-66. *Polym. Polym. Compos.* **2010**, *18*, 253–258. [[CrossRef](#)]
32. Sangeetha, V.; Kanagathara, N.; Sumathi, R.; Sivakumar, N.; Anbalagan, G. Spectral and Thermal Degradation of Melamine Cyanurate. *J. Mater.* **2013**, 262094. [[CrossRef](#)]
33. Tang, H.; Ng, K.; Chui, S.S.; Che, C.; Lam, C.; Yuen, K.; Siu, T.; Lan, L.C.; Che, X. Analysis of Melamine Cyanurate in Urine Using Matrix-Assisted Laser Desorption/Ionization Mass Spectrometry. *Anal. Chem.* **2009**, *81*, 3676–3682.
34. Kohl, M.; Alafid, F.; Bouška, M.; Krejčová, A.; Raycha, Y.; Kalendová, A.; Hrdina, R.; Burgert, L. New Corrosion Inhibitors Based on Perylene Units in Epoxy Ester Resin Coatings. *Coatings* **2022**, *12*, 923. [[CrossRef](#)]
35. Kohl, M.; Alafid, F.; Boštková, K.; Bouška, M.; Krejčová, A.; Svoboda, J.; Slang, S.; Michalčíková, L.; Kalendová, A.; Hrdina, R.; et al. New Azo Dyes-Based Mg Complex Pigments for Optimizing the Anti-Corrosion Efficiency of Zinc-Pigmented Epoxy Ester Organic Coatings. *Coatings* **2023**, *13*, 1276. [[CrossRef](#)]
36. Pareek, S.; Behera, D. Mixed metal oxides composites as corrosion inhibitors. In *Inorganic Anticorrosive Materials*; Elsevier: Amsterdam, The Netherlands, 2022; pp. 325–343.
37. Kar, J.K.; Stevens, R.; Bowen, C.R. Processing and characterization of various mixed oxide and perovskite-based pigments for high temperature ceramic colouring application. *J. Alloys Compd.* **2008**, *461*, 77–84. [[CrossRef](#)]

38. Hatami, L.; Jamshidi, M. Effects of type and duration of pigment milling on mechanical and colorimetric properties of colored self-compacting mortars (CSCM). *J. Build. Eng.* **2021**, *35*, 102006. [[CrossRef](#)]
39. Wang, J.; Xu, H.; Battocchi, D.; Bierwagen, G. The determination of critical pigment volume concentration (CPVC) in organic coatings with fluorescence microscopy. *Prog. Org. Coat.* **2014**, *77*, 2147–2154. [[CrossRef](#)]
40. Lobnig, R.E.; Villaba, W.; Vogelsang, J.; Schmidt, R.; Zanger, P.; Soetemann, J. Development of a new experimental method to determine critical pigment–volume–concentrations using impedance spectroscopy. *Prog. Org. Coat.* **2006**, *55*, 363–374. [[CrossRef](#)]
41. Kalendová, A. Alkalisising and neutralising effects of anticorrosive pigments containing Zn, Mg, Ca, and Sr cations. *Prog. Org. Coat.* **2000**, *38*, 199–206. [[CrossRef](#)]
42. Rodríguez, M.T.; Gracena, J.J.; Saura, J.J.; Suay, J.J. The influence of the critical pigment volume concentration (CPVC) on the properties of an epoxy coating: Part, I.I. Anticorrosion and economic properties. *Prog. Org. Coat.* **2004**, *50*, 68–74. [[CrossRef](#)]
43. Liang, J.-Z. Reinforcement and quantitative description of inorganic particulate-filled polymer composites. *Compos. Part B Eng.* **2013**, *51*, 224–232. [[CrossRef](#)]
44. Müller, B.; Fischer, S. Epoxy ester resins as corrosion inhibitors for aluminium and zinc pigments. *Corros. Sci.* **2006**, *48*, 2406–2416. [[CrossRef](#)]
45. Kalendová, A.; Veselý, D.; Kalenda, P. Contribution of inorganic pigments to the formation of paint films from oxypolymerising drying paints. *Pigment. Resin Technol.* **2010**, *39*, 255–261. [[CrossRef](#)]
46. Zhao, Y.; Wang, J.; Pan, A.; He, L.; Simon, S. Degradation of red lead pigment in the oil painting during UV aging. *Color Res. Appl.* **2019**, *44*, 790–797. [[CrossRef](#)]
47. Arul, K.; Thanigai, E.; Manikandan, J.; Ramya, R.; Indira, K.; Mudali, U.K.; Henini, M.; Asokan, K.; Dong, C.; Kalkura, S.N. Enhanced anticorrosion properties of nitrogen ions modified polyvinyl alcohol/Mg-Ag ions co-incorporated calcium phosphate coatings. *Mater. Chem. Phys.* **2021**, *261*, 124182. [[CrossRef](#)]
48. Nguyen, J.; Akdemiz, A.; Anuso, C.L.; Morris, J.D. A Simple At-Home Titration: Quantifying Citric Acid in Lemon Juice with Baking Soda and Mentos. *J. Chem. Educ.* **2023**, *100*, 739–744. [[CrossRef](#)]
49. Zhang, X.; Feng, Z.; Xie, J.; Guo, H.; Zhou, K.; Li, C.; Ma, J.; Wang, X.; Xu, K.; Liu, J. Corrosion inspired inhibitor releasing for BTA@ZIF-8 modified epoxy coatings in seawater environment. *Colloids Surf. A Physicochem. Eng. Asp.* **2023**, *673*, 131866. [[CrossRef](#)]
50. Kalendová, A. Effects of particle sizes and shapes of zinc metal on the properties of anticorrosive coatings. *Prog. Org. Coat.* **2003**, *46*, 324–332. [[CrossRef](#)]

Disclaimer/Publisher’s Note: The statements, opinions and data contained in all publications are solely those of the individual author(s) and contributor(s) and not of MDPI and/or the editor(s). MDPI and/or the editor(s) disclaim responsibility for any injury to people or property resulting from any ideas, methods, instructions or products referred to in the content.